

Blank page

## Acknowledgements

(*Lời cảm ơn*)

Trong quá trình thực hiện luận văn này, tôi xin gửi lời cảm ơn đến những người đã hỗ trợ giúp đỡ mình trong suốt thời gian qua.

Đầu tiên, tôi xin gửi lời cảm ơn đến thầy Nguyễn Tân Tiến, người đã hướng dẫn tôi thực hiện nghiên cứu đề tài này, tạo điều kiện để tôi có thể tham gia dự án thực tế về Humanoid robot, tham gia các hội nghị khoa học trong lĩnh vực nghiên cứu để tích lũy và trao đổi kiến thức chuyên môn.

Tiếp theo, lời cảm ơn xin được gửi tới thành viên của Hi-Tech Lab hỗ trợ tôi trong việc góp ý, trao đổi trong công việc, giúp tôi thiết kế modun ZMP được sử dụng trong luận văn này.

Cuối cùng tôi xin cảm ơn đến quý thầy trong bộ môn Cơ điện tử đã truyền đạt kiến thức cho tôi xuyên suốt từ đại học đến thời điểm thực hiện luận văn này.

Tp Hồ Chí Minh, 17 tháng 6 năm 2017

Nguyễn Văn Tiến Anh

## **Abstract**

This thesis presents the study on walking control of biped robot based on humanoid robot UXA-90. The forward and inverse kinematics of 12 DoF biped robot were solved, a simulation tool also developed to implement walking gait. The experiment results show that robot can be stable walking by using the gait was designed.

## **Tóm tắt**

Luận văn này trình bày phương pháp hoạch định quỹ đạo cho chuyển động đi hai chân của Humanoid robot và áp dụng lên robot UXA-90. Dựa trên thông số động học của robot này, bài toán động học thuận và ngược của hai chân robot 12 DoF đã được giải quyết, một mô hình mô phỏng đã được xây dựng. Kết quả thực nghiệm cho thấy quỹ đạo hoạch định có thể làm robot đi ổn định.

## **Declaration**

This thesis is a presentation of my original research work. Wherever contributions of others are involved, every effort is made to indicate this clearly, with due reference to the literature, and acknowledgement of collaborative research and discussions.

Nguyễn Văn Tiên Anh

## Table of Contents

Acknowledgements .....	i
Abstract.....	ii
Declaration.....	iii
Table of Contents.....	iv
List of Figures.....	vii
List of Tables .....	ix
List of Abbreviations .....	x
CHAPTER 1: INTRODUCTION .....	1
1.1    Adult-sized humanoid robot .....	1
1.1.1    WABIAN series of Waseda University .....	1
1.1.2    Honda Humanoid robot.....	2
1.1.3    HRP series of AIST/KAWADA .....	3
1.1.4    HUBO series of KAIST .....	4
1.1.5    Boston Dynamics Humanoid robot.....	5
1.1.6    NASA's Humanoid robot.....	6
1.2    Child-sized humanoid robot.....	7
1.2.1    Nao Humanoid robot.....	7
1.2.2    iCub Humanoid robot.....	8
1.2.3    DARwIn-OP Humanoid robot .....	8
1.2.4    UXA-90 Humanoid robot .....	9
1.3    Humanoid walking.....	10
1.3.1    Introduction to human walking gait .....	10

1.3.2	Humanoid robot walking pattern generation .....	11
1.3.3	The stability of biped walking.....	12
1.4	Overview of the Thesis .....	14
CHAPTER 2: BIPED ROBOT: MODELING AND KINEMATICS .....		15
2.1	Modeling of biped robot .....	15
2.1.1	The Zero Moment Point .....	15
2.1.2	Calculating ZMP .....	17
2.1.3	The Linear Inverted Pendulum Model. ....	18
2.1.4	The Cart-Table Model.....	21
2.2	Kinematics of biped robot.....	22
2.2.1	Forward kinematic .....	23
2.2.2	Inverse kinematic .....	29
CHAPTER 3: CONTROL OF WALKING GAIT .....		32
3.1	CoM trajectory .....	32
3.1	Ankle trajectory .....	35
CHAPTER 4: SIMULATION AND EXPERIMENT .....		37
4.1	Simulation .....	37
4.2	Experiment on UXA-90 robot .....	39
4.2.1	ZMP module.....	39
4.2.2	Experiment results and discussion .....	40
CHAPTER 5: CONCLUSION .....		43
5.1	Remark of UXA-90.....	43
5.2	Contributions of thesis .....	44
5.3	Recommendations for future research .....	44

References .....	46
Appendix A: MATLAB code .....	48
Appendix B: UXA-90 datasheet.....	51
Publications .....	53

## List of Figures

Figure 1.1 Wabian-2 humanoid robot .....	1
Figure 1.2 Honda humanoid robots .....	2
Figure 1.3 HRP humanoid robots.....	4
Figure 1.4 Humanoid robots of KAIST.....	5
Figure 1.5 Boston Dynamics humanoid robots .....	6
Figure 1.6 Valkyrie humanoid robot .....	7
Figure 1.7 NAO humanoid robot.....	8
Figure 1.8 DARwIn-OP humanoid robot .....	9
Figure 1.9 UXA-90 humanoid robot .....	9
Figure 1.10 Human walking cycle [16].....	10
Figure 1.11 CoM, ZMP, and Support Polygon [18].....	11
Figure 1.12 The approaches used for generating walking patterns of biped robot [19]	11
Figure 1.13 ZMP stability [17].....	13
Figure 2.1 Biped mechanism and forces acting on its sole .....	15
Figure 2.2 The ground reaction forces $f_i = [f_{ix} \ f_{iy} \ f_{iz}]^T$ at the discretized points $p_i = [p_{ix} \ p_{iy} \ p_{iz}]^T$ .....	16
Figure 2.3 Schematic 3D Biped model and ZMP at P .....	17
Figure 2.4 The 3D-LIMP .....	19
Figure 2.5 The Cart-Table model .....	21
Figure 2.6 Basic parameters of UXA-90.....	22
Figure 2.7 The coordination of biped robot .....	23
Figure 2.8 The coordinates on let leg .....	25
Figure 2.9 The coordinates on right leg.....	26

Figure 2.10 Characterization of generic link <i>i</i> .....	28
Figure 2.11 Inverse kinematic algorithm.....	29
Figure 2.12 Inverse kinematic of a singular posture. ....	31
Figure 3.1 Pattern generation as ZMP tracking control .....	32
Figure 3.2 ZMP reference and CoM trajectory on <i>x</i> direction.....	34
Figure 3.3 ZMP reference and CoM trajectory on <i>y</i> direction.....	34
Figure 3.4 Footstep planning, ZMP reference and CoM trajectory in <i>xy</i> plan.....	35
Figure 3.5 Ankle trajectories design with $La0 = Ds/2$ , $Ha0 = 0.03 m$ , $Lan = l5$ ....	35
Figure 3.6 Walking gait of 4 steps with single support, double support, swing, stance phase time are: $Tss = 0.56 s$ , $Tds = 0.14 s$ , $Tsw = 0.56 s$ , $Tst = 0.84 s$ .....	36
Figure 4.1 The block diagram of biped robot walking simulation.....	37
Figure 4.2 Joints position during walk .....	38
Figure 4.3 Configuration of 4 sensors on each foot .....	39
Figure 4.4 Attachment of each sensor include: (1) Contact point; (2) Foot plate 1; (3) Rigid plate 1; (4) Rigid plate 2; (5) Flexi Force A401 sensor; (6) Foot plate 2.....	39
Figure 4.5 Magnitude of pressure.....	40
Figure 4.6 Implement walking gait on real robot .....	41
Figure 4.7 Simulation and experiment result of ZMP .....	41
Figure 5.1 System schematic of robot UXA-90 .....	43
Figure 5.2 ROS software is being developed by author.....	45
Figure A.1 The binary tree of robot link .....	48
Figure A.2 UXA-90 specifications.....	51
Figure A.3 SAM-30 and SAM-100P specifications.....	52
Figure A.4 SAM-160P and SAM-210P specifications .....	52

## **List of Tables**

Table 1.1 The methods of the pattern generators for biped walking [20].	12
Table 2.1 Modified Denavit-Hartenberg parameter of the legs .....	24

## **List of Abbreviations**

CoM	Center of Mass
CoP	Center of Pressure
DoF	Degree of Freedom
DSP	Double Support Phase
SSP	Single Support Phase
ZMP	Zero-Moment Point
3D LIPM	3D Linear Inverted Pendulum Model
ROS	Robot Operating System

## CHAPTER 1: INTRODUCTION

During the past three decades research, development of robotics has expanded from traditional industrial robot manipulators to include autonomous and animal-like or humanoid robots. The field of humanoid robotics is concerned with the creation of robots which are broadly human-like in their behavior, their morphology or both. Building truly humanoid robots will require significant advances in areas including high-level cognition, computer vision, speech synthesis, speech recognition, manipulation and biped locomotion.

Over the past two decades, the field of humanoid robotics has witnessed significant advances and many humanoid robots project have been developed.

### 1.1 Adult-sized humanoid robot

#### 1.1.1 WABIAN series of Waseda University

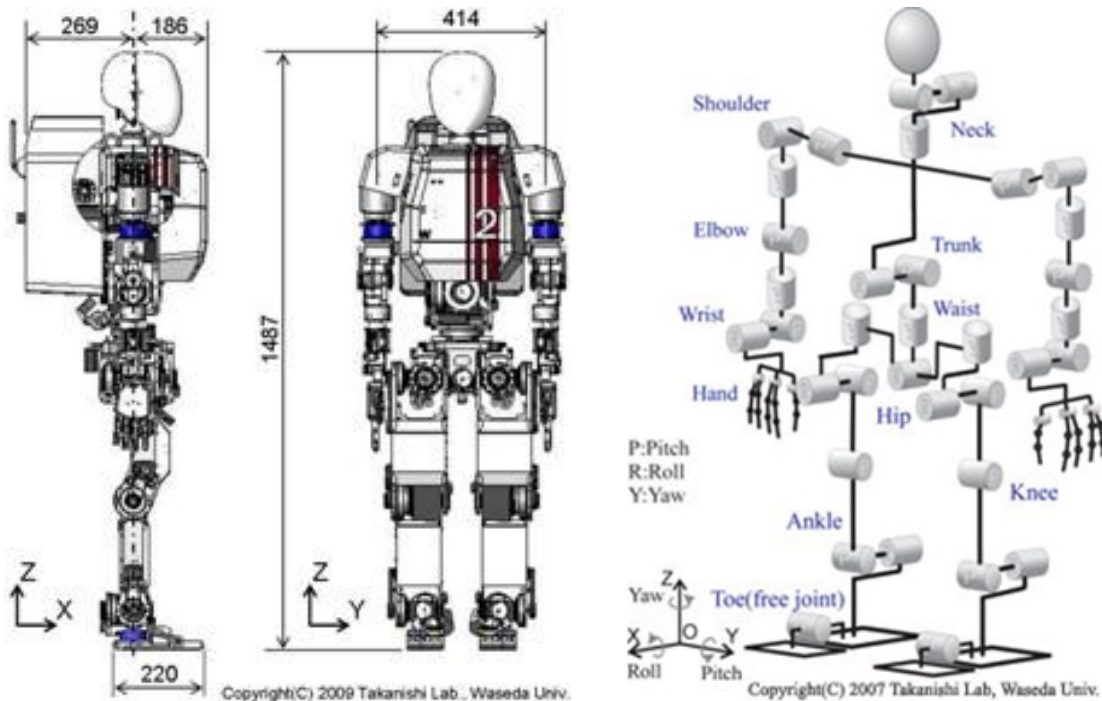


**Figure 1.1** Wabian-2 humanoid robot

The first humanoid research was performed by Kato and Tsuiki at Waseda University in Japan in 1972. This research realized a static walking by a heavy model:

WL-5 a three-dimensional, 11 DoF<sup>1</sup> walker [1]. The WL-5 was used as the lower limbs of the WABOT-1 [2] which is the first full-scale anthropomorphic robot developed in the world. It consisted of a limb-control system, a vision system and a conversation system.

The WABOT-1 was able to communicate with a person in Japanese and to measure distances and directions to the objects using external receptors, artificial ears and eyes, and an artificial mouth. The WABOT-1 walked with its lower limbs and was able to grip and transport objects with hands that used tactile sensors.

In 1984, the research group developed WABOT-2, a robot capable of performing on musical instruments with a capability equivalent to that of a professional musician.

In 2006, WABIAN-2 was released [3]. Its trunk is designed in order to permit rotation, and forward, backward, and side-way movement. Further, its arms are designed to support its complete weight when pushing a walk assist machine. Moreover, it can lean on a walk-assist machine by forearm control using trunk motion.

### 1.1.2 Honda Humanoid robot

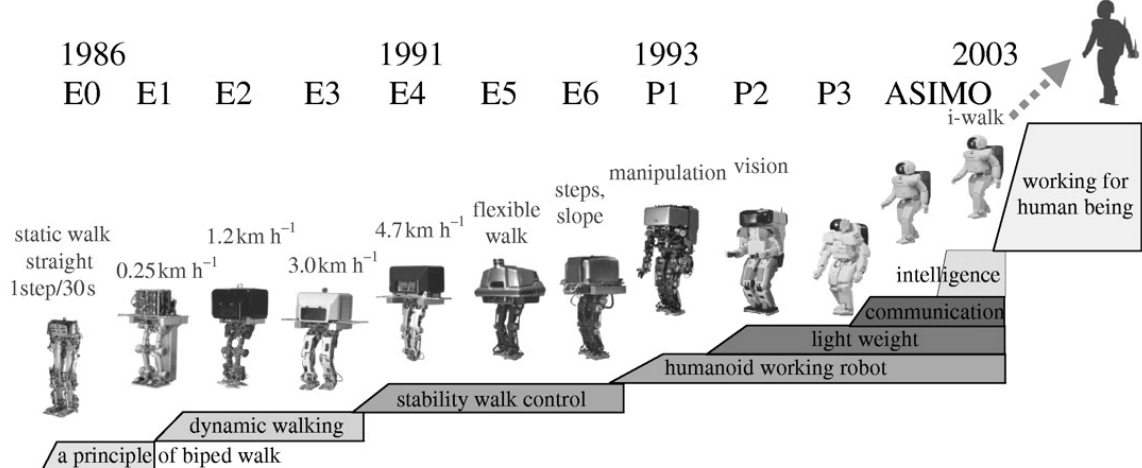


**Figure 1.2** Honda humanoid robots

Honda has been doing research on robotics since 1986, the research started with straight and static walking of biped robot [4], [5]. In December 1996, they announced

---

<sup>1</sup> Degree of Freedom

the world's first self-regulating two-legged humanoid robot P2. It has 182 [cm] tall, weighs 210 [kg] with total 34 of DoF. Because heavy, it has operational time of only 15 min and can walk on an uneven floor.

In 2000, Honda introduced ASIMO<sup>1</sup>. ASIMO can both walk and run (at speeds of up to 3 [km/h]), and the current version incorporates a total of 57 DoF. ASIMO can also walk up and down stairs, and perform dance routines. ASIMO weighs 48 [kg] and its height is 130 [cm]. ASIMO can walk in a straight line, on a circle, turn and even slalom, enabling ASIMO to operate in most common human environments. As well as improving the complexity of its walking direction.

### *1.1.3 HRP<sup>2</sup> series of AIST/KAWADA*

The HRP is a project for development of general domestic helper robot in Japan. This project is spearheaded by Kawada Industries and supported by the National Institute of Advanced Industrial Science and Technology (AIST) and Kawasaki Heavy Industries, Inc.

In 1997, the project released robot HRP-1, this robot was developed based on Honda P3 robot. HRP-1 has been used for investigating the applications of a humanoid robot for the maintenance task of industrial plants and security services of home and office [6]. After that, the project developed HRP-1S robot. In this robot, they combined Honda P3 hardware and AIST controller. Its legs and arms are controlled separately and not suitable for some application [7].

In phase two of HRP (2000 - 2002), they developed a new humanoid robotics platform HPR-2. First, they developed two modules of robot: HPR-2L (leg module) and HPR-2A (arm module). The ability of the biped locomotion of HPR-2L is better than HPR-1, it can walk on uneven surface, walking speed up to 2.5 [km/h]. The arm module was designed for cooperative task with a human. Then they developed the whole-body humanoid base on two modules above and it is called HRP-2P. Finally, the project refined HRP-2P at various points the released humanoid robot platform HRP-2 in 2002.

---

<sup>1</sup> Advanced Step in Innovative MObility

<sup>2</sup> Humanoid Robotics Project

An interesting feature that HRP-2 has is the ability to stand up again after lying flat on the floor either on its back or front. Something that Honda's ASIMO is not able to do.

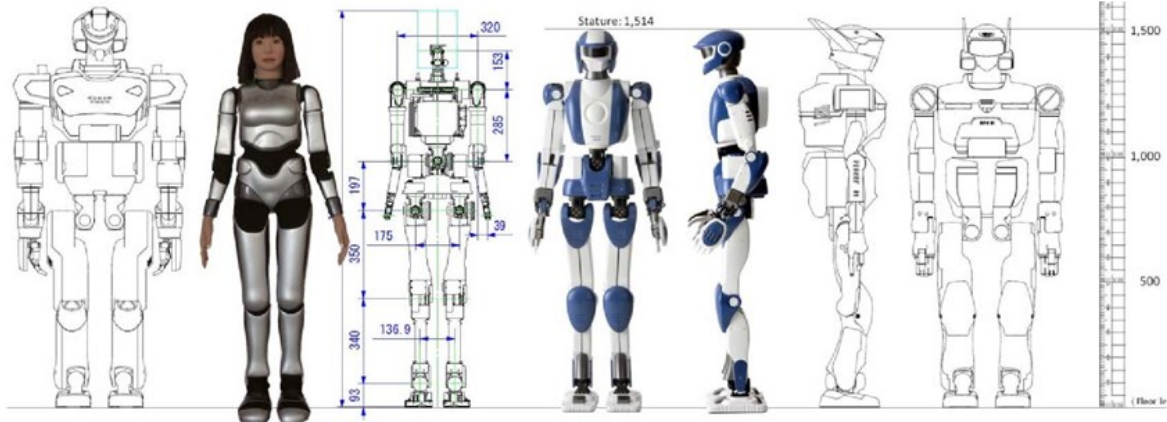


**Figure 1.3** HRP humanoid robots

In 2007, new humanoid robot of HRP was released, HRP-3, which stands for Humanoid Robotics Platform-3. HRP-3 is a human-size humanoid robot. Its main mechanical and structural components are designed to prevent the penetration of dust or spray [8].

The latest HRP robot series is HRP-4, it has a total of 34 DoF, including 7 DoF for each arm to facilitate object handling and has a slim, lightweight body with a height of 151 [cm] and weighs 39 [kg] [9].

#### 1.1.4 *HUBO series of KAIST*<sup>1</sup>

This research was inspired, in part, by Honda's newly unveiled ASIMO [10]–[12]. In 2000, KHR-0, the bipedal robot without arms or an upper body was developed by a laboratory in KAIST. The KHR-1 robot followed in 2003 and KHR-2, which was fully humanoid in shape, with a head and functioning hands, followed in 2004. The KHR-3, then titled HUBO, was developed and in 2005 in order to celebrate the 100th anniversary of the announcement of the theory of special relativity.

KAIST and Hanson Robotics joined forces to create Albert HUBO, a Humanoid Robots, Their Simulators, and the Reality Gap variant of the KHR-3, with the addition

---

<sup>1</sup> Korea Advanced Institute of Science and Technology

of a realistic animatronic head modeled on the famous scientist. This added head allowed for the generation of a variety of expressions emulating surprise, happiness, sadness, etc.

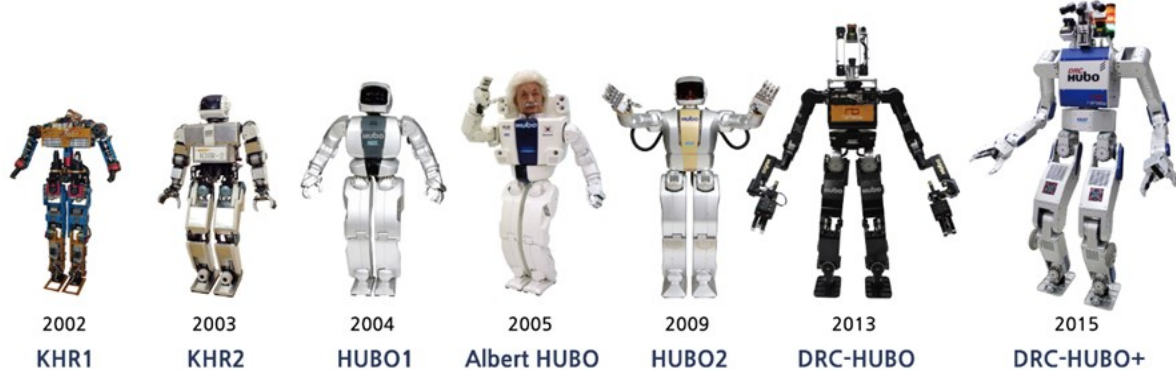


**Figure 1.4** Humanoid robots of KAIST

The HUBO2 robot, also known as KHR-4 was developed in 2009, and has a total of 40 DoF. It has a height of 125 [cm], weighs 45 [kg] and is capable of walking at 1.5 [km/h], running at 3.6 [km/h]. HUBO2++ is a variant of HUBO2, taking into account issues of user convenience (Heo et al. 2012).

Variants of HUBO2 were entered by two teams for the United States Defense Advanced Research Projects Agency (DARPA) robotics challenge, team DRC-HUBO based at Drexel University, and Team KAIST.

### 1.1.5 Boston Dynamics Humanoid robot

In 2013, one of the most impressive humanoid robots in existence at the present time is the Atlas humanoid robot, developed by the American company Boston Dynamics. This robot was based on Petman robot.

Petman uses hydraulic actuation to produce the large range of motion and high strength required for natural human-like behavior. It weighs about 80 [kg] with an additional payload capacity of 23 [kg], is 140 [cm] tall at the shoulder and has an outside body form that closely conforms to a 50th percentile male and has a total of 29 DoF. PETMAN is able to walk at speeds up to 4.8 [km/h] [13].

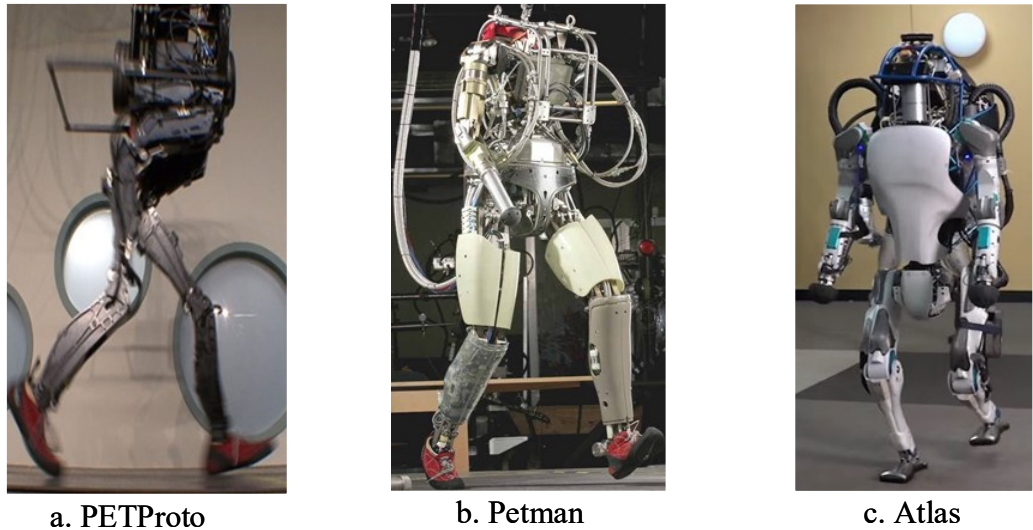


**Figure 1.5** Boston Dynamics humanoid robots

Atlas has 180 [cm] tall and weighs 150 [kg] with a total of 28 DoF [14]. February 23, 2016, Boston Dynamics released new version of Atlas, it was designed to operate both outdoors and inside buildings. It is specialized for mobile manipulation and is very adaptive at walking over a wide range of under grounds including snow.

#### 1.1.6 NASA's Humanoid robot

Valkyrie is the first NASA's bipedal humanoid robot [15], NASA adopted a long range approach and developed Valkyrie with the ultimate goal of creating a robotic platform that is capable and effective in both space and Earth-bound applications.

The Valkyrie effort represents numerous advancements in robotics in the areas of rotary series elastic joints, embedded motion control, energy storage, embedded computing, distributed control, pressure based tactile sensing, supervisory control, operator interface design and electric motor research.

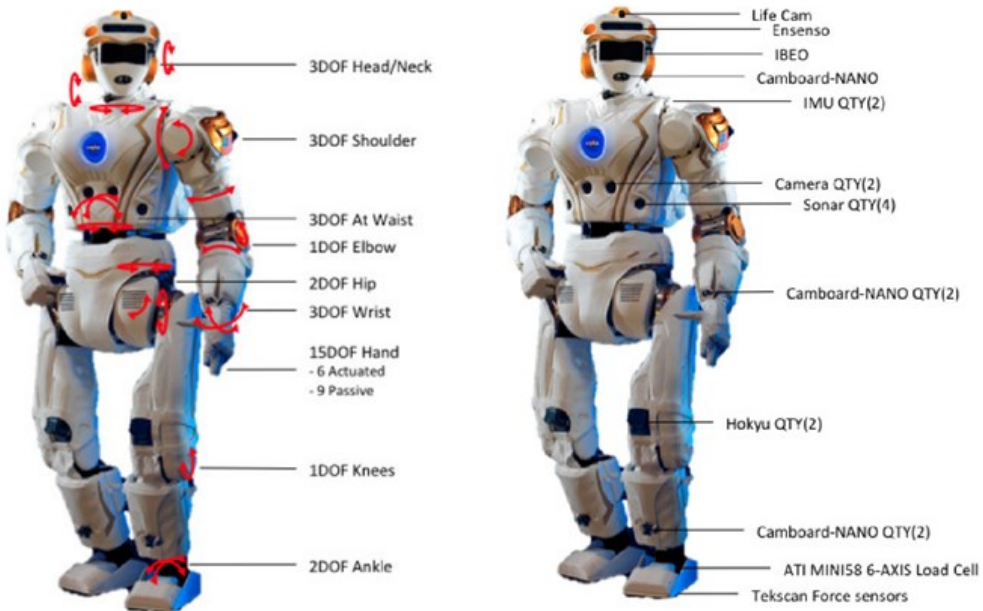


**Figure 1.6** Valkyrie humanoid robot

Valkyrie stands 187 [cm] tall, weighs 129 [kg], with a total of 44 DoF and approximates a human range of motion.

## 1.2 Child-sized humanoid robot

Humanoid robots have size of a child are low cost and the best choice for research and education project.

### 1.2.1 Nao Humanoid robot

Nao humanoid robot is manufactured by Aldebaran robotics, it has total 21 DoF (model used for RoboCup competition), weight 4.3 [kg] and height 58 [cm] (model Nao NextGen).

Nao can dance generation, omni-directional walking for RoboCup applications, humanoid robot walking and comparing three different learning algorithms.

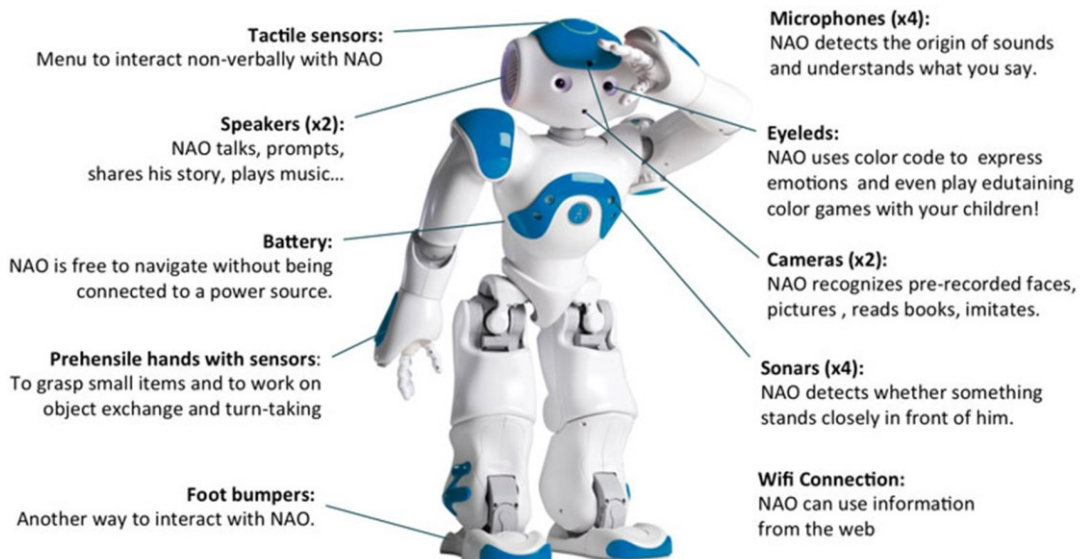


**Figure 1.7 NAO humanoid robot**

### 1.2.2 *iCub Humanoid robot*

The iCub is the humanoid robot developed at IIT as part of the EU project RoboCup and subsequently adopted by more than 20 laboratories worldwide. It has 53 DoF in total that move the head, arms & hands, waist, and legs. iCub robot has height 105 [cm] and weight 24 [kg].

It can see and hear, furthermore it has the sense of proprioception and movement (using accelerometers and gyroscopes). They are working to improve on this in order to give the iCub the sense of touch and to grade how much force it exerts on the environment.

### 1.2.3 *DARwIn-OP<sup>1</sup>Humanoid robot*

DARwIn-OP is an affordable, miniature-humanoid-robot platform with advanced computational power, sophisticated sensors, high payload capacity, and dynamic motion ability to enable many exciting research and education activities. DARwIn-OP has total 20 DoF, height 455 cm and weight 2.8 kg.

---

<sup>1</sup> Dynamic Anthropomorphic Robot with Intelligence–Open Platform



**Figure 1.8** DARwIn-OP humanoid robot

#### 1.2.4 UXA-90 Humanoid robot

UXA-90 Humanoid Robot is a well-proportioned 100 [cm] tall humanoid shaped robot, it has been designed with a structure similar to the ratio of the ideal human body. UXA-90 is used in education research such as: Human Robot Interaction, Artificial intelligence, Humanoid robot competition. It has total 23 DoF (12 DoF of legs, 8 DoF of arms, 2 DoF of head and 1 DoF of wrist), weighs 9.5 [kg] and walking maximum speed at 30 [cm/s].

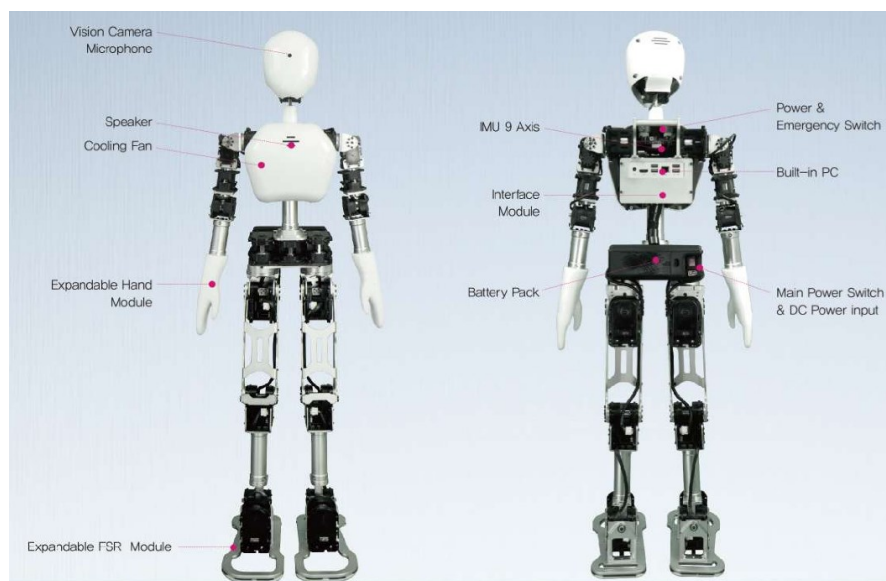


**Figure 1.9** UXA-90 humanoid robot

### 1.3 Humanoid walking

#### 1.3.1 Introduction to human walking gait

The complete gait cycle of human walking consists of two main successive phases: the DSP<sup>1</sup> and the SSP<sup>2</sup> with intermediate sub-phases. The DSP arises when both feet contact the ground resulting in a closed chain mechanism, while the SSP starts when the rear foot is not supported by the ground with the front foot flatting on the ground. One should note that the percentage of DSP is about 20% of time during one stride of the gait cycle whereas SSP is about 80% of time.

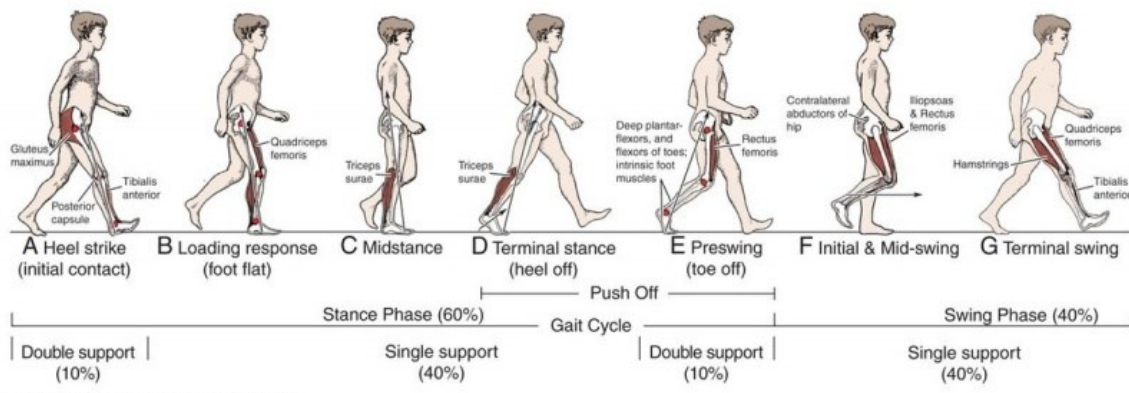


**Figure 1.10** Human walking cycle [16]

One of the goals of implementing this humanoid walking controller is achieve a walking gait that is more human-like. In order to achieve this, the human gait is presented and then simplified to match the needs of the controller. During walking, at least one foot remains in contact with the ground at all times.

#### Notions

*Center of Mass (CoM)*: is as one might imagine, the equivalent center of collection of mass bearing particles. It can be calculated by averaging the position of each particle and weighing it by its mass.

*Zero Moment Point (ZMP)*: is the point on the ground where the net moment vector of the inertial and gravitational forces of the entire body has zero components in horizontal planes [17]

<sup>1</sup> Double Support Phase

<sup>2</sup> Single Support Phase

*Support Polygon (SP):* is formed by the convex hull about the floor support points.

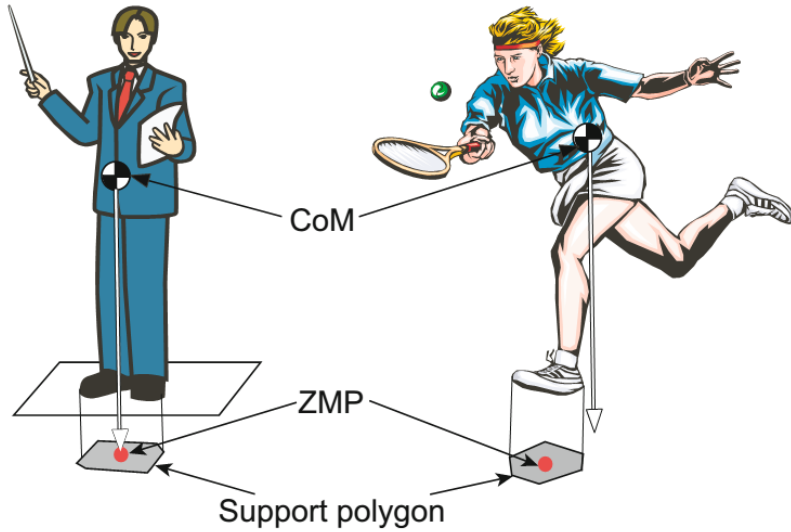


**Figure 1.11** CoM, ZMP, and Support Polygon [18]

### 1.3.2 Humanoid robot walking pattern generation

One of the important issues of the humanoid walking is the generation of the desired paths that ensure stability while avoiding collision with obstacles. Due to the similarity between the humanoid robot and the human locomotion, some important aspects should be considered in order to generate natural biped locomotion, which are as follows:

- Learning (training), which needs a certain level of intelligence.
- A high level of adaptability to cope with uneven terrains and external disturbances.
- In specific circumstances, optimal motion to reduce energy consumption during walking.

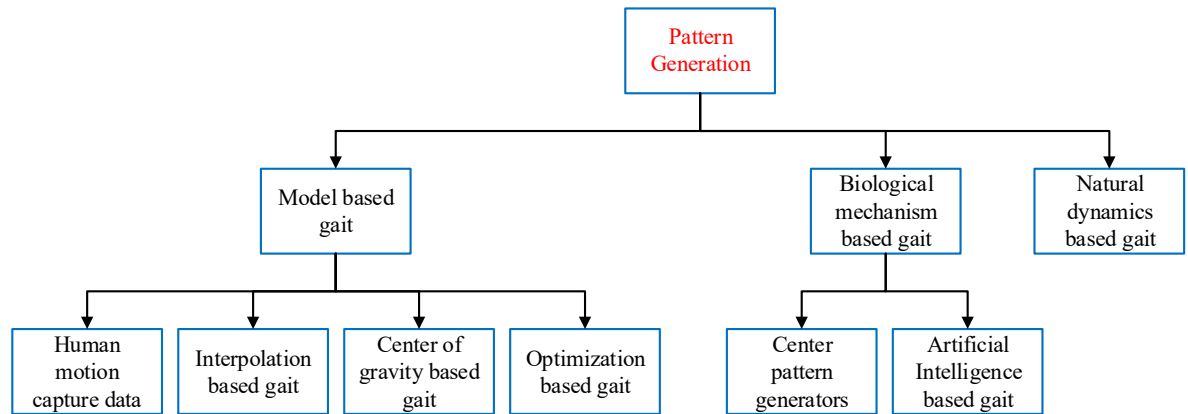


**Figure 1.12** The approaches used for generating walking patterns of biped robot [19]

**Table 1.1** The methods of the pattern generators for biped walking [20].

<i>The approach</i>	<i>Advantages</i>	<i>Disadvantages</i>
Model based gait	<ul style="list-style-type: none"> <li>• It provides explanations about the behavior of human walking.</li> <li>• It can adopt ZMP and periodicity as stability criteria. Consequently, it can guarantee the dynamic stability of biped mechanism.</li> </ul>	<ul style="list-style-type: none"> <li>• It needs full knowledge of the dynamic model of biped robot.</li> <li>• The online walking algorithms require large computations.</li> <li>• It rarely employs the natural dynamics of the biped system.</li> <li>• Information of the motion terrain should be known.</li> </ul>
Biological mechanism based gait	<ul style="list-style-type: none"> <li>• It does not need precise modeling of biped mechanism.</li> <li>• Online walking algorithms could be applied easily.</li> <li>• It is robust to disturbances.</li> <li>• It can guarantee the stability of biped mechanism.</li> </ul>	<ul style="list-style-type: none"> <li>• The limitations of CPG are widely investigated.</li> <li>• Significant results are obtained without explanations.</li> </ul>
Natural dynamic based gait	<ul style="list-style-type: none"> <li>• It employs the natural dynamics of the biped.</li> <li>• Less energy consumption could be produced.</li> <li>• It can produce natural motion.</li> </ul>	<ul style="list-style-type: none"> <li>• No unified strategies could be adopted to achieve the desired results.</li> <li>• All strategies depend on the experiences of the designer.</li> </ul>

### 1.3.3 The stability of biped walking

Stability analysis of biped walking is difficult, since dynamics of the biped robots are highly non-linear, under actuated, subject to impacts, variable external forces, and discrete changes between different modes. The common strategies, such as analysis of the eigenvalues, gain and phase margins or Lyapunov stability theory, can be applied to particular modes, such as a single or double stance, but are usually incapable to characterize stability of all modes in total [21]. In general, there are two techniques to analysis stability of biped walking gait: ZMP criterion and Poincare return map which were applied to most biped walking controller of humanoid robot.

## ZMP criterion

If ZMP is located inside the support polygon then the system is stable and unstable if the ZMP is outside the SP.

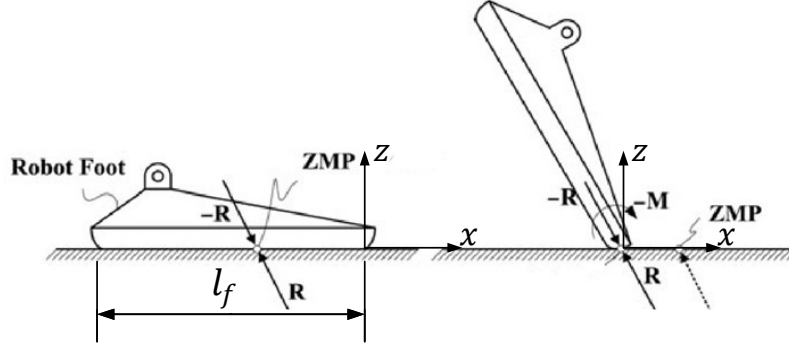


**Figure 1.13** ZMP stability [17]

The necessary associated constraint is:

$$-l_f \leq x_{ZMP}(t) \leq 0 \quad (1.1)$$

## Poincare return map

The biped robots based on periodic stability can perform cyclic sequences of steps that are stable as a whole, but not locally at every instance of time. The Poincare return map is used to show the stability of this type of walking as described below [22].

The transition of the current biped state  $v_k$  to the successive state after one walking step  $v_{k+1}$  can be described by the stride function  $S$  as follows:

$$v_{k+1} = S(v_k) \quad (1.2)$$

Orbital stability is investigated by using a perturbation around the initial fixed point

$$S(v_f + \Delta v) \approx v_f + P\Delta v \quad (1.3)$$

where  $P = \frac{\partial S}{\partial v}$  denotes the linear return matrix which governs the orbital stability of the biped robot.

- If the eigenvalues of  $P$  are within the unit circle of the complex plane, the biped system is stable, otherwise it is unstable

## 1.4 Overview of the Thesis

We can notice that almost humanoid projects are started from biped walking research such as: Wabian, Honda, Boston Dynamic humanoid robot... or start from humanoid robot platform such as: HRP project. At the initial step in humanoid robot research, study on bipedal walking is very important because this is a specific.

Thus, my thesis focuses on research the walking of humanoid robot. There are two main problems in thesis: designing biped walking gait and modeling biped robot.

- Designing biped walking gait: create reference trajectory for CoM, stance and swing leg ensure walking stable.
- Modeling biped robot: solving forward, inverse kinematic of biped robot and controller design for biped walking gait.

## CHAPTER 2: BIPED ROBOT: MODELING AND KINEMATICS

In this chapter, the models for walking of biped robot are explained. The forward kinematics and inverse kinematics of a biped robot with 12 DoF are solved by using Denavit – Hartenberg convention.

### 2.1 Modeling of biped robot

Biped robots, an open kinematic chain, are complex in design. It has numerous DoF due to the goal of mimicking the human gait. To study on the stability of the system, many researchers have simplified the biped robot model. LIPM and Cart-table are two simple models applied in design and control of biped robot walking. These models find the relationship between CoM and ZMP, CoM describes the position of robot and ZMP describes the state of robot (stable or unstable).

#### 2.1.1 The Zero Moment Point

For biped locomotion, the Zero Moment Point is one of the most used and famous terms, it is widely known by the acronym ZMP. Originally, it was defined by Vukobratovic et al. in 1972 [23].

ZMP is defined as that point on the ground at which the net moment of the inertial forces and the gravity forces has no component along the horizontal axes.

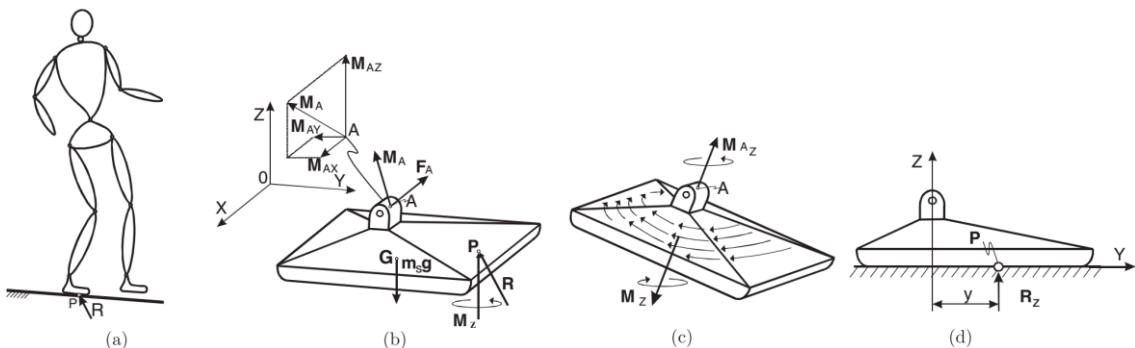


**Figure 2.1** Biped mechanism and forces acting on its sole

If  $P$  is a ZMP position, it will have properties  $\tau_x^P = 0$  and  $\tau_y^P = 0$ . Position of  $P$  can be determined by solving equation was proposed in [17]

$$(\overrightarrow{OP} \times \vec{R})^H + \overrightarrow{OG} \times m_s g + M_A^H + (\overrightarrow{OA} \times \vec{F}_A)^H = 0 \quad (2.1)$$

where the parameters show in Figure 3.2.

For flat ground contact of our support foot with the floor the ZMP corresponds with the position of the CoP<sup>1</sup>. The CoP (and in flat ground contact the ZMP) of an object in contact with the ground can be computed as the sum of all contact points  $p_1, \dots, p_n$  weighted by the forces in z direction  $f_{1z}, \dots, f_{nz}$  that is applied

$$\mathbf{p} = \begin{bmatrix} p_x \\ p_y \\ p_z \end{bmatrix} = \frac{\sum_{i=1}^n p_i f_{iz}}{\sum_{i=1}^n f_{iz}} \quad (2.2)$$

The distributed  $n$  force vectors are replaced by a force and a moment vectors acting at the CoP as

$$\mathbf{f} = \sum_{i=1}^n f_i \quad (2.3)$$

$$\boldsymbol{\tau} = \sum_{i=1}^n (p_i - \mathbf{p}) \times \mathbf{f}_i \quad (2.4)$$

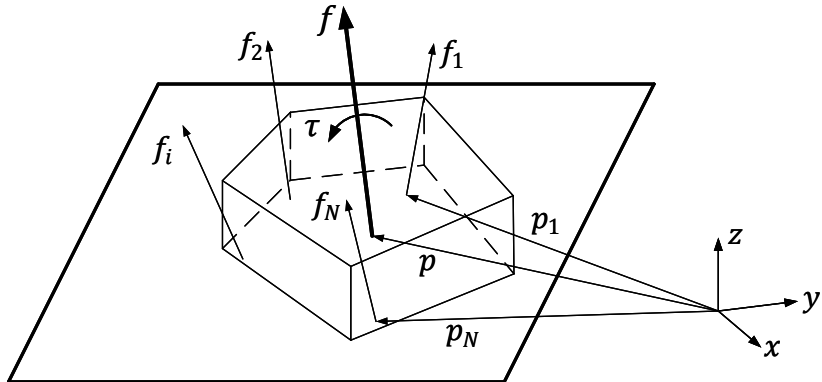


**Figure 2.2** The ground reaction forces  $\mathbf{f}_i = [f_{ix} \ f_{iy} \ f_{iz}]^T$  at the discretized points  $\mathbf{p}_i = [p_{ix} \ p_{iy} \ p_{iz}]^T$

Because ground contact is flat, so we have  $p_{iz} = 0, p_z = 0$ . Splitting equation (2.4) along  $x$  and  $y$  axis

$$\tau_x = \sum_{i=1}^n p_{iy} f_{iz} - p_y \sum_{i=1}^n f_{iz} \quad (2.5)$$

---

<sup>1</sup> Center of Pressure

$$\tau_y = - \sum_{i=1}^n p_{ix} f_{iz} + p_x \sum_{i=1}^n f_{iz} \quad (2.6)$$

The ZMP position can be calculated easily by set  $\tau_x = 0$  and  $\tau_z = 0$ .

## ZMP Criterion

In order to achieve a dynamically stable gait the ZMP should be within the support polygon, at every time instance.

### 2.1.2 Calculating ZMP

This section implements procedure to calculate ZMP of multibody model in simulation, the model is given in Figure 2.3.

**Step 1:** Calculate the total mass of robot  $M$

$$M = \sum_{i=0}^n m_i \quad (2.7)$$

**Step 2:** Calculate the position of CoM  $p_{CoM} = [x \ y \ z]^T$

$$p_{CoM} = \frac{\sum_{i=0}^n m_i p_i}{M} \quad (2.8)$$

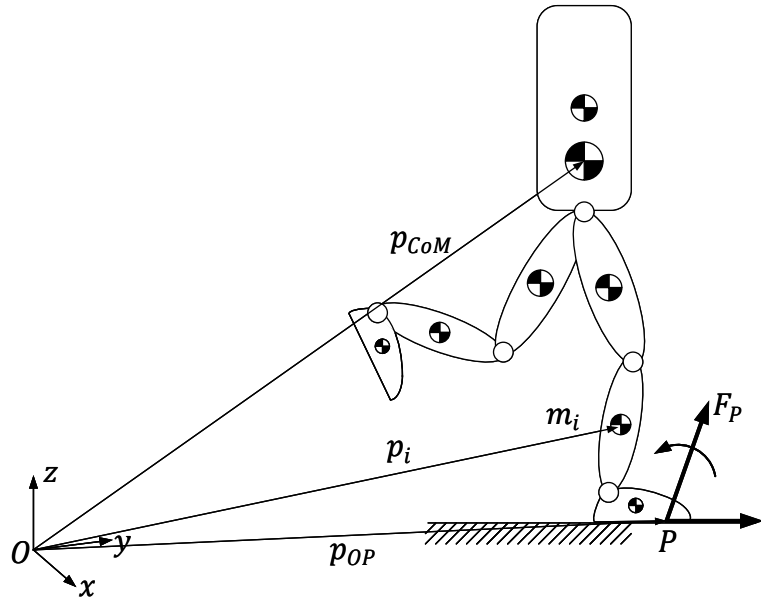


**Figure 2.3** Schematic 3D Biped model and ZMP at P

**Step 3:** Calculate the total linear momentum  $P$  and the total angular momentum  $\mathcal{L}$

$$P = \sum_{i=0}^n m_i \dot{p}_i \quad (2.9)$$

$$\mathcal{L} = \sum_{i=0}^n p_i \times m_i \dot{p}_i + I_i \omega_i \quad (2.10)$$

where  $I_i$  and  $\omega_i$  are inertia tensor and the angular velocities of the  $i$ -th link with respect to the base frame origin. Because matrix  $I_i$  is respect to the base frame origin, it is calculated by

$$I_i = {}^W R_i \mathbb{I}_i {}^W R_i^T \quad (2.11)$$

with  $\mathbb{I}_i$  is the inertia matrix of the  $i$ -th link w.r.t. the link frame origin attached to their links

**Step 4:** The position of ZMP in  $x, y$  direction can be computed

$$p_x = \frac{Mgx + p_z \dot{P}_x - \dot{\mathcal{L}}_y}{Mg + \dot{P}_z} \quad (2.12)$$

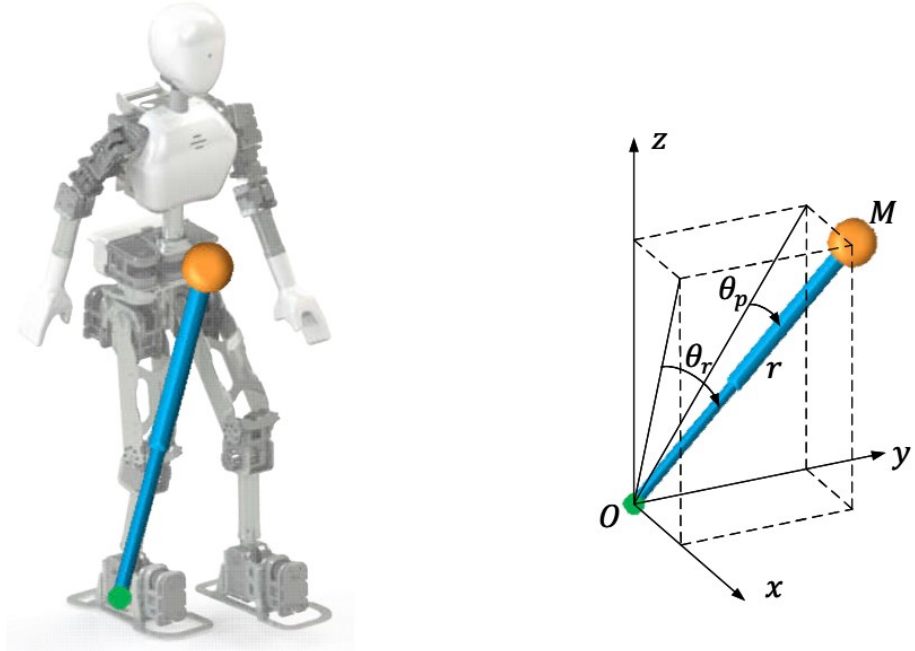
$$p_y = \frac{Mgy + p_z \dot{P}_y + \dot{\mathcal{L}}_x}{Mg + \dot{P}_z} \quad (2.13)$$

Remind that is the  $p_z$  height of the floor, when robot walks on flat floor  $p_z = 0$ .

### 2.1.3 The Linear Inverted Pendulum Model.

A simple model for describing the dynamics of a bipedal robot during single support phase is the 3D inverted pendulum. We reduce the body of the robot to a point-mass at the center of mass.

The support leg is replaced by a mass-less telescopic leg which is fixed at a point on the supporting foot. Initially this will yield non-linear equations that will be hard to control. However, by constraining the movement of the inverted pendulum to a fixed plane, we can derive a linear dynamic system. This model is called the 3D Linear Inverted Pendulum Model (3D LIPM) [24].

**Figure 2.4** The 3D-LIMP

This model assumes that the base of the base of the pendulum is fixed at the origin of the current Cartesian coordinate system. The position of pendulum is  $p = [x \ y \ z]^T$  with mass  $M$  equals the total weight of the robot. The position of  $M$  is uniquely specified by a set of state variables  $q = [\theta_r \ \theta_p \ r]^T$ .

$$\begin{aligned} x &= rS_p \\ y &= -rS_r \\ z &= rD \end{aligned} \tag{2.14}$$

where  $S_r = \sin \theta_r$ ,  $S_p = \sin \theta_p$ ,  $D = \sqrt{1 - S_r^2 - S_p^2}$ .

From which we can compute the Jacobian by partial derivation

$$J = \frac{\partial p}{\partial q} = \begin{bmatrix} 0 & rC_p & S_p \\ -rC_r & 0 & -S_r \\ -rC_rS_r/D & -rC_pS_p/D & D \end{bmatrix} \tag{2.15}$$

where  $C_p = \cos \theta_p$ ,  $C_r = \cos \theta_r$ .

Let  $[\tau_r, \ \tau_p, \ f]$  be the actuator torque and force associated with the state variables  $[\theta_r \ \theta_p \ r]$ . With these inputs, the equation of motion of the 3D inverted pendulum is given

$$M \begin{bmatrix} \ddot{x} \\ \ddot{y} \\ \ddot{z} \end{bmatrix} = (J^T)^{-1} \begin{bmatrix} \tau_r \\ \tau_p \\ f \end{bmatrix} + \begin{bmatrix} 0 \\ 0 \\ -Mg \end{bmatrix} \tag{2.16}$$

We can describe the 3D Inverted Pendulum along the  $x$ -axis and  $y$ -axis by combining equations (2.14), (2.15) and (2.16)

$$M(z\ddot{x} - x\ddot{z}) = \frac{D}{C_p}\tau_p + Mgx \quad (2.17)$$

$$M(-z\ddot{y} + y\ddot{z}) = \frac{D}{C_r}\tau_r - Mgy \quad (2.18)$$

In order to linearize general nonlinear equations (2.14), the basic assumption that the CoM will have a constant displacement with regard to our ground plane. Thus, CoM moves on a plane that is parallel to the ground plane.

We are going to constrain the  $z$ -coordinate of our inverted pendulum to a plane with normal vector  $[k_x, k_y, -1]$  and  $z$ -displacement  $z_c$

$$z = k_x x + k_y y + z_c \quad (2.19)$$

The second derivative of  $z$  can be described by

$$\ddot{z} = k_x \ddot{x} + k_y \ddot{y} \quad (2.20)$$

Substituting (2.19) and (2.20) in to the equations (2.17) and (2.18) yields the following equations

$$\ddot{x} = \frac{g}{z_c}x + \frac{k_x}{z_c}(x\ddot{y} - \ddot{x}y) + \frac{1}{Mz_c}u_p \quad (2.21)$$

$$\ddot{y} = \frac{g}{z_c}y - \frac{k_x}{z_c}(x\ddot{y} - \ddot{x}y) - \frac{1}{Mz_c}u_r \quad (2.22)$$

Where  $u_r$ ,  $u_p$  are the virtual inputs which are introduced to compensate input nonlinearity.

$$\tau_r = \frac{C_r}{D}u_r \quad (2.23)$$

$$\tau_p = \frac{C_p}{D}u_p \quad (2.24)$$

When robot walks on flat floor  $k_x = 0, k_y = 0$ , equations (2.21) and (2.22) become simplification

$$\ddot{x} = \frac{g}{z_c}x + \frac{1}{Mz_c}u_p \quad (2.25)$$

$$\ddot{y} = \frac{g}{z_c}y - \frac{1}{Mz_c}u_r \quad (2.26)$$

We can easily calculate the ZMP of 3D LIPM

$$\begin{aligned} p_x &= -\frac{u_p}{Mg} \\ p_y &= \frac{u_r}{Mg} \end{aligned} \quad (2.27)$$

By substituting equation (2.27) to (2.25) and (2.26) we obtain the relationship between CoM and ZMP position

$$\begin{aligned} \ddot{x} &= \frac{g}{z_c}(x - p_x) \\ \ddot{y} &= \frac{g}{z_c}(y - p_y) \end{aligned} \quad (2.28)$$

#### 2.1.4 The Cart-Table Model

The Cart-Table model is used to compute the resulting ZMP from an CoM motion. The model consists of an infinitely large mass-less table of height  $z_c$ , while the foot of the table has the shape of the support polygon.

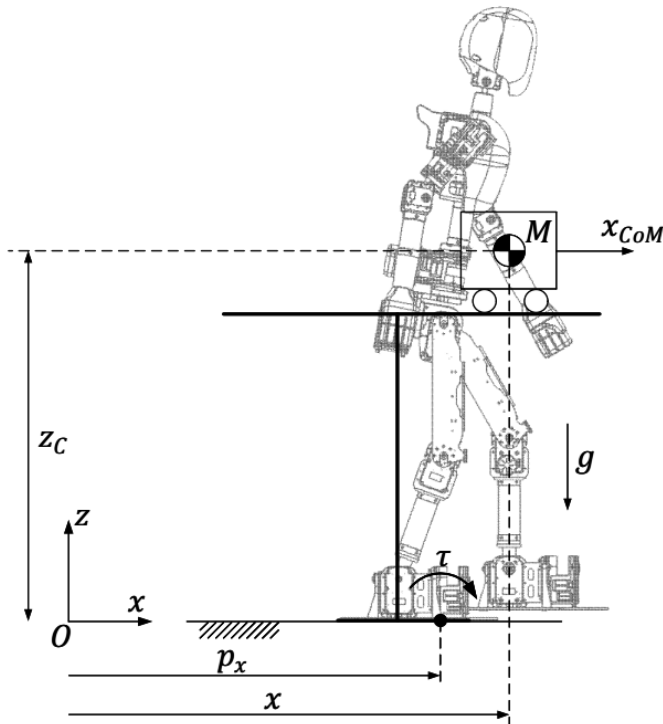


**Figure 2.5** The Cart-Table model

Given a frictionless cart with mass  $M$  at position  $p_{CoM} = [x \ y \ z_c]^T$  that move on the table we can compute the resulting ZMP in  $p = [p_x \ p_y \ p_z]^T$  the support foot. Please note that the 3D-dimensional model is equivalent to having two independent tables with

two carts each in the  $xz$  and  $yz$  plane respectively. First of all, lets compute the torque  $\tau_x$  and  $\tau_y$  around the  $x$ -axis and  $y$ -axis at ZMP on the support foot.

In this case, the torque  $\tau$  around point P can be written as

$$\tau_y = -Mg(x - p_x) + M\ddot{x}z_c \quad (2.29)$$

By using the ZMP definition:  $\tau_y = 0$ , the ZMP position in  $x$  direction is calculated

$$p_x = x - \frac{z_c}{g} \ddot{x} \quad (2.30)$$

For the  $y$  direction the derivation is similar

$$p_y = y - \frac{z_c}{g} \ddot{y} \quad (2.31)$$

## 2.2 Kinematics of biped robot

In order to control a biped robot, the forward and inverse kinematic solutions are required. The solution to this problem involves solving for the joint angles given a desired position and orientation while accounting for singularities, joint limits and feasible workspace issues.

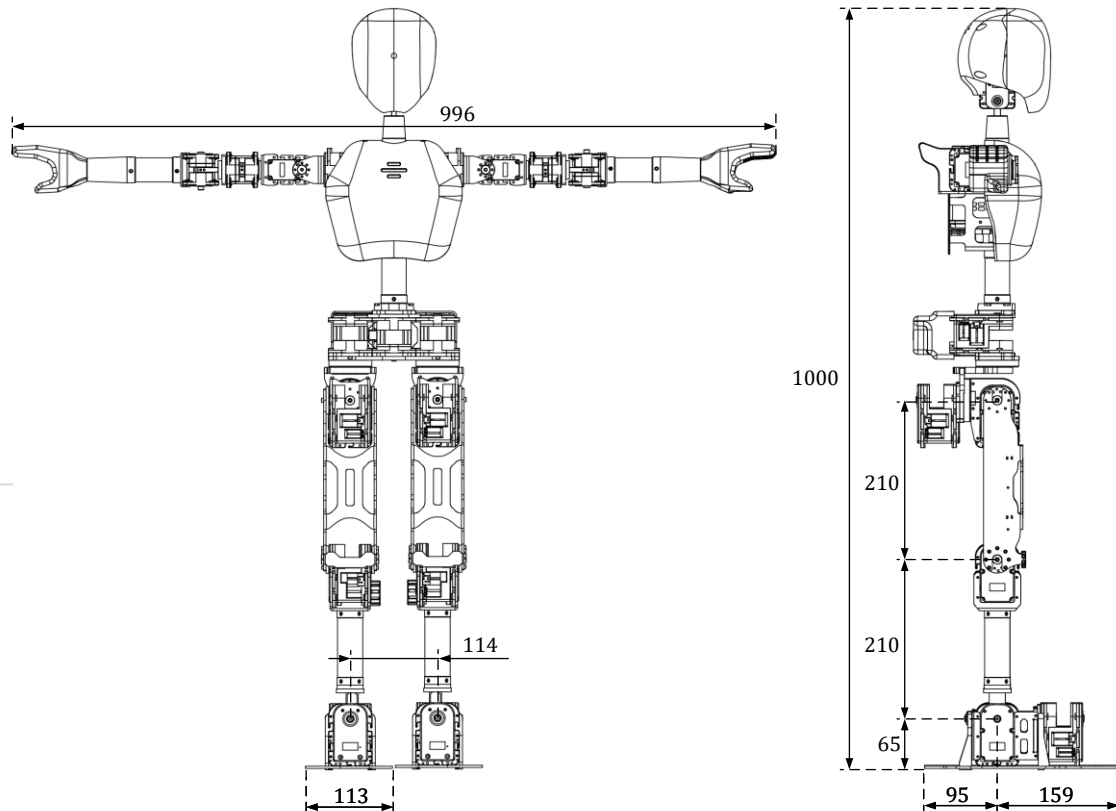


**Figure 2.6** Basic parameters of UX-90

This thesis uses the parameters of UXA-90 legs, Figure 2.6 shows mechanical dimension of UXA-90 robot.

### 2.2.1 Forward kinematic

The forward kinematics transforms the kinematic information of a robot joint-link from the joint space to the Cartesian space. The most common method is to apply the Denavit Hartenberg (DH) transformation. The coordinate system of biped robot is given in Figure 2.7,  $O_1$  and  $O_0$  are robot and world coordinate. There are two kinematic chains in biped robot mechanism

Left leg :  $O_1 \rightarrow O_2 \rightarrow O_3 \rightarrow O_4 \rightarrow O_5 \rightarrow O_6 \rightarrow O_7$

Right leg :  $O_1 \rightarrow O_8 \rightarrow O_9 \rightarrow O_{10} \rightarrow O_{11} \rightarrow O_{12} \rightarrow O_{13}$

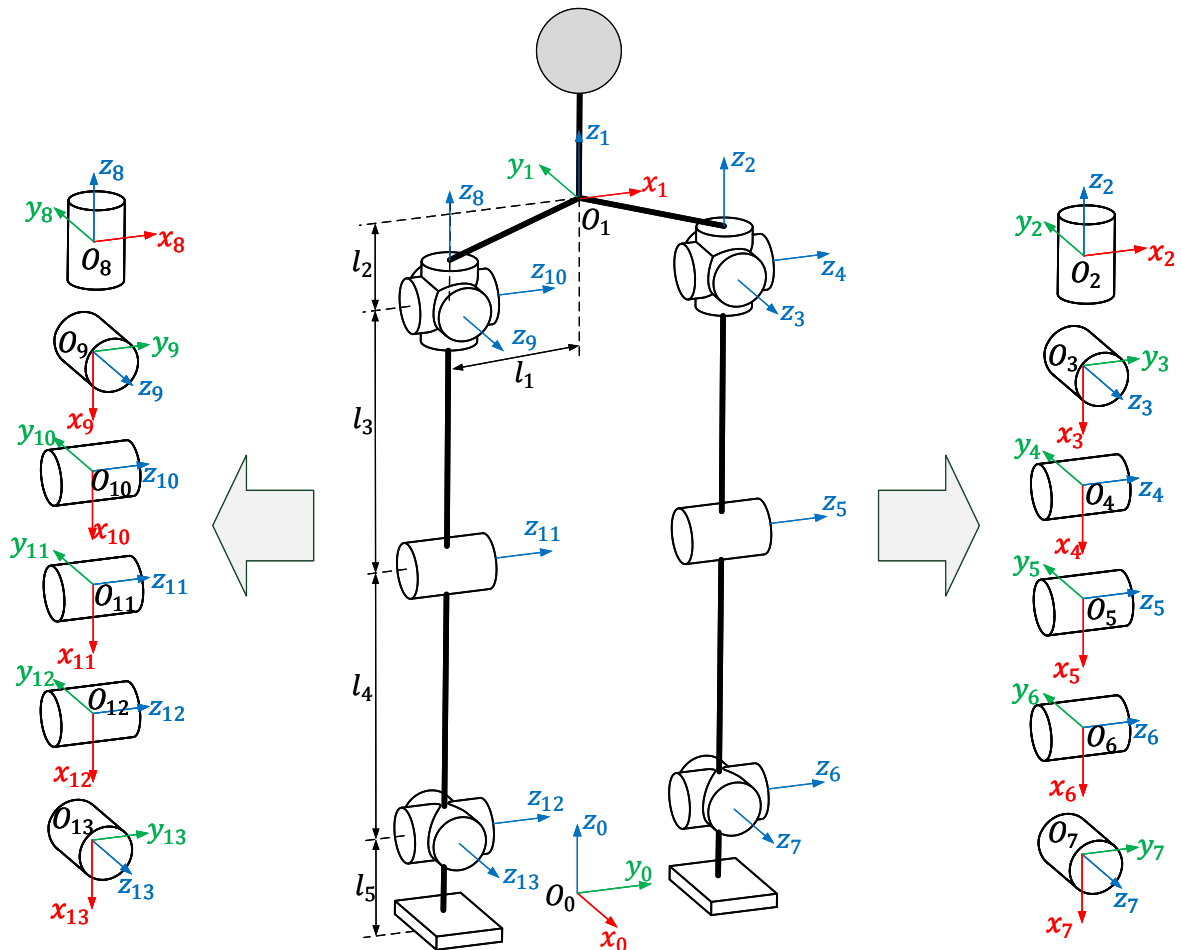


**Figure 2.7** The coordination of biped robot

The kinematic structure of the right and left side of biped robot are identical, therefore, the left and right legs have the same joint coordinate frames and Modified Denavit-Hartenberg (DH) parameters shows in Table 2.1.

**Table 2.1** Modified Denavit-Hartenberg parameter of the legs

$i$	$q_i$	$\alpha_i$	$a_i$	$d_i$
1			${}^0T_1$	
2	$q_2$	0	$l_1$	$-l_2$
3	$q_3 - \pi/2$	$\pi/2$	0	0
4	$q_4$	$-\pi/2$	0	0
5	$q_5$	0	$l_3$	0
6	$q_6$	0	$l_4$	0
7	$q_7$	$\pi/2$	0	0
8	$q_8$	0	$-l_1$	$-l_2$
9	$q_9 - \pi/2$	$\pi/2$	0	0
10	$q_{10}$	$-\pi/2$	0	0
11	$q_{11}$	0	$l_3$	0
12	$q_{12}$	0	$l_4$	0
13	$q_{13}$	$\pi/2$	0	0

While :  $l_1 = 0.057m$ ,  $l_2 = 0.042m$   $l_3 = l_4 = 0.21m$ ,  $l_5 = 0.065m$ .

Figure 2.8 and Figure 2.9 shows the coordinate of links on right leg

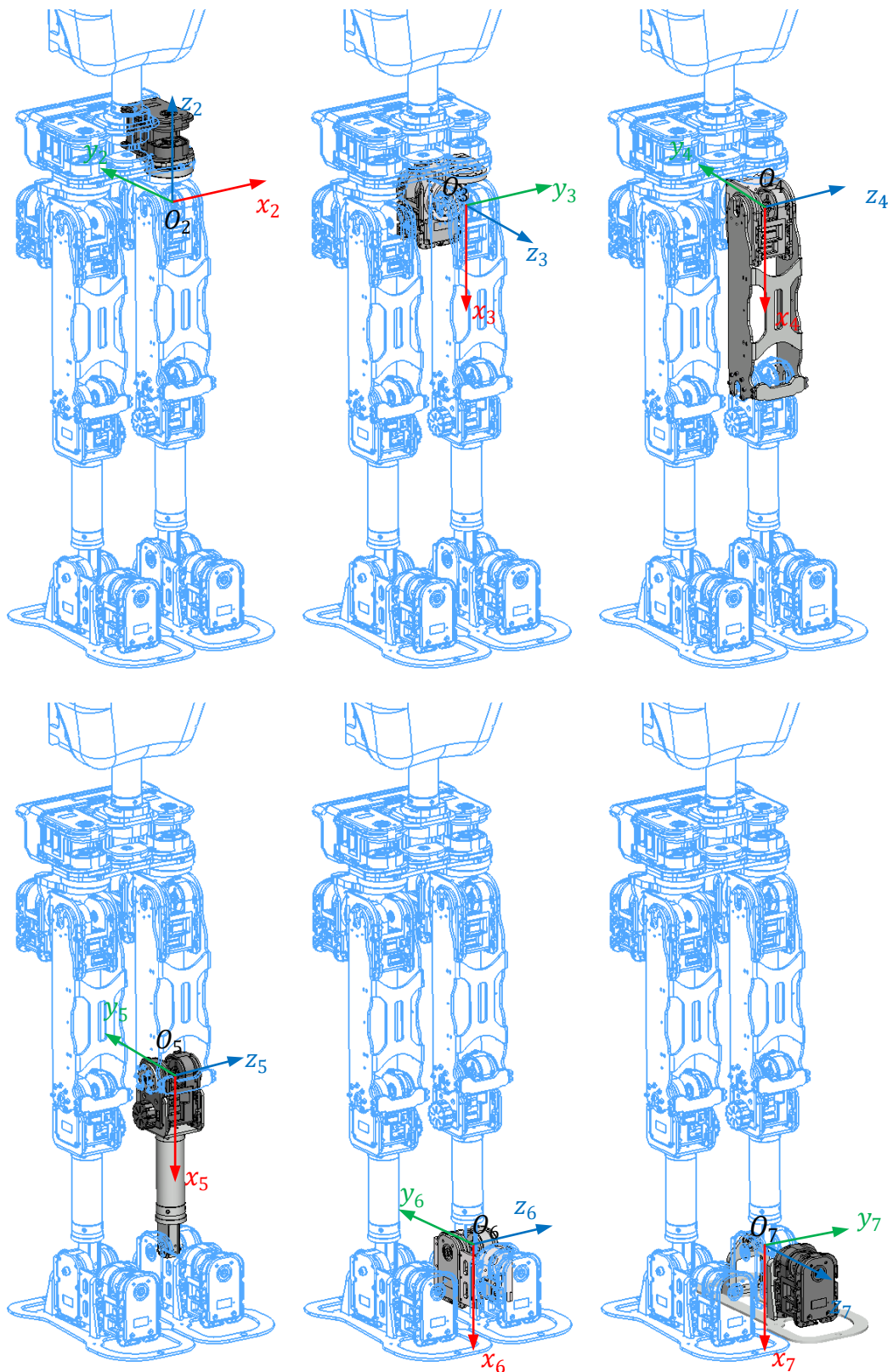


**Figure 2.8** The coordinates on let leg

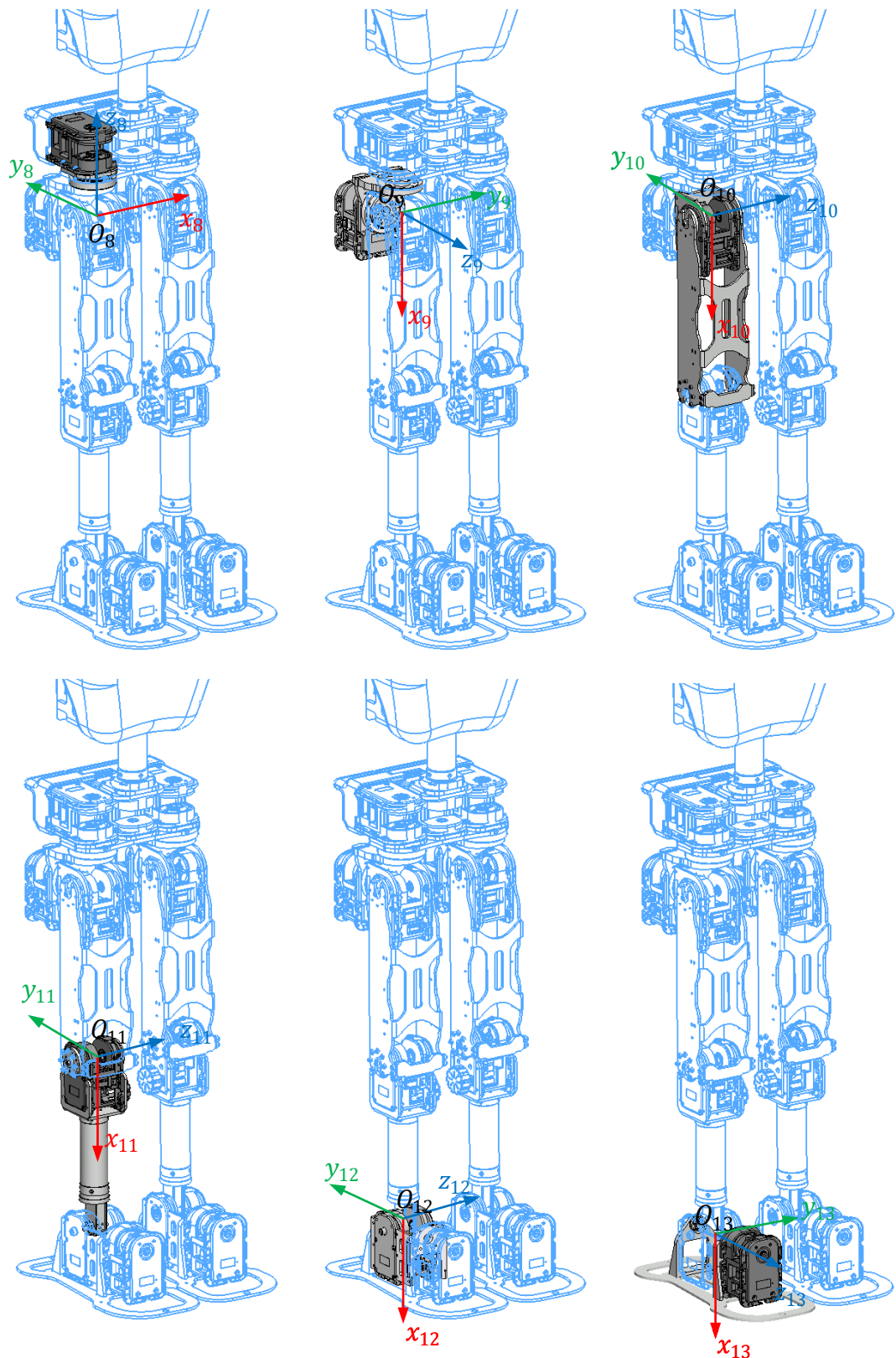


**Figure 2.9** The coordinates on right leg

According to the modified D-H convention, the homogeneous transformation from coordinate  $i - 1$  to  $i$  is given by matrix  ${}^{i-1}T_i$

$${}^{i-1}T_i = \begin{bmatrix} \cos \theta_i & -\sin \theta_i & 0 & a_i \\ \cos \alpha_i \sin \theta_i & \cos \alpha_i \cos \theta_i & -\sin \alpha_i & -d_i \sin \alpha_i \\ \sin \alpha_i \sin \theta_i & \sin \alpha_i \cos \theta_i & \cos \alpha_i & d_i \cos \alpha_i \\ 0 & 0 & 0 & 1 \end{bmatrix} \quad (2.32)$$

Equation (2.32) can be wrote

$${}^{i-1}T_i = \begin{bmatrix} {}^{i-1}R_i & {}^{i-1}p_i \\ 0 & 1 \end{bmatrix} \quad (2.33)$$

The forward kinematic equation of left leg is (2.34) and right leg is (2.35)

$$LFK(q) = {}^wT_0 \prod_{i=2}^7 {}^{i-1}T_i = \begin{bmatrix} n_L & s_L & a_L & p_L \\ 0 & 0 & 0 & 1 \end{bmatrix} \quad (2.34)$$

$$RFK(q) = {}^wT_0 \prod_{i=8}^{13} {}^{i-1}T_i = \begin{bmatrix} n_R & s_r & a_R & p_R \\ 0 & 0 & 0 & 1 \end{bmatrix} \quad (2.35)$$

## Velocities

Let  ${}^0p_{i-1}$  and  ${}^0p_i$  be the position vector of the origins of frame  $i - 1$  and  $i$  in world coordinate (Figure 2.10).

The angular velocity it is calculated

$${}^0\omega_i = {}^0\omega_{i-1} + \dot{q}_i z_i \quad (2.36)$$

The linear velocity it is calculated

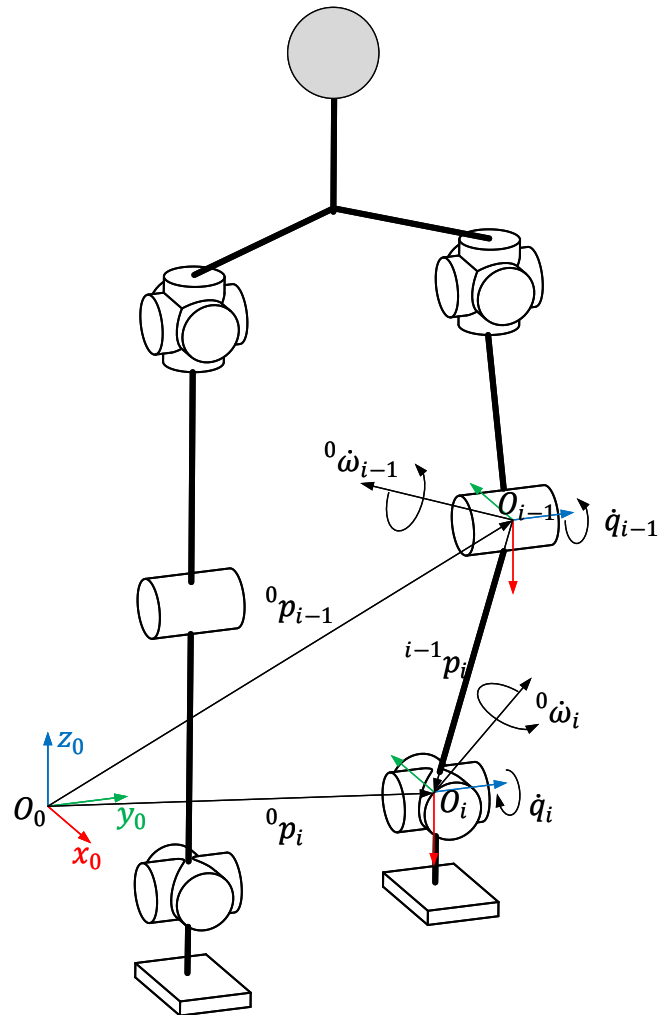
$${}^0\dot{p}_i = {}^0\dot{p}_{i-1} + {}^0\omega_{i-1} \times {}^0R_{i-1} {}^{i-1}p_i \quad (2.37)$$

## Jacobian matrix

Jacobian is a matrix which provides the relationship between the end-effector velocities and the joint velocities. This matrix is required in some inverse kinematics algorithms.

$$\dot{x}_e = \begin{bmatrix} \dot{p}_e \\ \omega_e \end{bmatrix} = \begin{bmatrix} J_P \\ J_O \end{bmatrix} \dot{q} \quad (2.38)$$

where  $\dot{p}_e$  and  $\omega_e$  are the linear and angular velocity of end-effector,  $\dot{q}$  is joint velocity,  $J_P$  is the matrix relating the contribution of the  $\dot{q}$  to  $\dot{p}_e$  while  $J_O$  is the matrix relating the contribution of the  $\dot{q}$  to  $\omega_e$ .

**Figure 2.10** Characterization of generic link  $i$ 

The Jacobian matrix is given  $J(q) = [J_P \ J_O]^T$ , method to find it was proposed in [25, Ch. 3]. Let us rewrite Jacobian matrix as form

$$J = \begin{bmatrix} j_{P1} & \dots & j_{Pn} \\ j_{O1} & \dots & j_{On} \end{bmatrix} \quad (2.39)$$

Each column of  $J$  is calculated by

$$\begin{bmatrix} j_{Pi} \\ j_{Qi} \end{bmatrix} = \begin{cases} \begin{bmatrix} z_{i-1} \\ 0 \end{bmatrix} & \text{for a prismatic joint} \\ \begin{bmatrix} z_{i-1} \times (p_e - p_{i-1}) \\ z_{i-1} \end{bmatrix} & \text{for a revolute joint.} \end{cases} \quad (2.40)$$

$z_{i-1}$  is given by the third column of the rotation matrix  ${}^0 R_{i-1}$

$p_e$  is given by the first three elements of the fourth column of the transformation matrix  ${}^0 T_e$ .

$p_{i-1}$  is given by the first three elements of the fourth column of the transformation matrix  ${}^0T_{i-1}$ .

For a given configuration  $q$ , we can view the Jacobian as a linear transformation mapping joint velocities  $\dot{q}$  to link  $i$  velocities  $\dot{x}_i = [\dot{p}_i \ \omega_i]^T$

$$\dot{x}_i = \sum_1^i \begin{bmatrix} j_{Pi} \\ j_{Oi} \end{bmatrix} \begin{bmatrix} q_1 \\ \vdots \\ q_i \end{bmatrix} \quad (2.41)$$

### 2.2.2 Inverse kinematic

By considering (2.38), the joint velocities can be obtained via simple inversion of the Jacobian matrix

$$\dot{q} = J^{-1}(q)\dot{x}_e \quad (2.42)$$

The integration can be performed in discrete time by resorting to numerical techniques.

$$\Delta q = J^{-1}(q)\Delta x_e \quad (2.43)$$

Let us call  ${}^d p$ ,  ${}^d R = [n_d \ s_d \ a_d]$  are position, rotation matrix desired of end-effector and  $p$ ,  $R = [n \ s \ a]$  are current position and rotation matrix of end-effector, the error posture is defined

$$e = \begin{bmatrix} {}^d p - p \\ \frac{1}{2}(n \times n_d + s \times s_d + a \times a_d) \end{bmatrix} = \begin{bmatrix} [e_x \ e_y \ e_z]^T \\ [e_{roll} \ e_{pitch} \ e_{yaw}]^T \end{bmatrix} \quad (2.44)$$

The inverse kinematic in robotics is find joint position from end-effector posture. The numerical techniques are used when robot has many DOF. Figure 2.11 shows the Newton Raphson algorithm to solve inverse kinematic

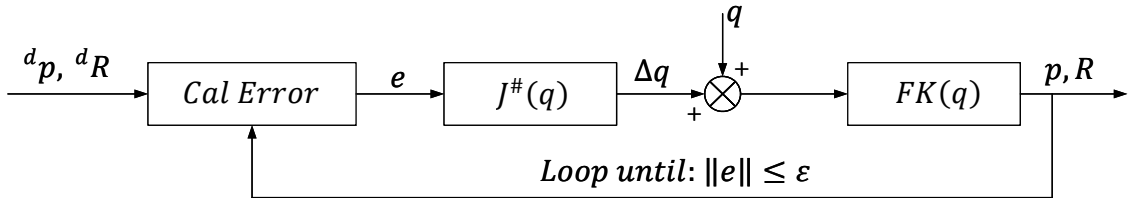


**Figure 2.11** Inverse kinematic algorithm.

According to the method, if Jacobian matrix is full rank  $J^\#(q) = J^{-1}(q)$ . When robot legs are in singular posture, Jacobian loses its rank, the inverse of  $J(q)$  becomes ill-conditioned and the solution (2.42) tends to infinity the task cannot be executed.

To handle the singularities, we use the damped least-squares method was proposed in [26]. This method compromises the requirement of accuracy in tracking the end-effector trajectory in order to obtain feasible joint velocities. One way of posing the damped least-squares problem is to minimize the sum of the norm of the residual error in the task space  $\|\dot{x}_e + J\dot{q}\|$ , and the norm of the joint velocity vector  $\|\dot{q}\|$ . The most general form in which the problem can be given

$$\min\{\|\dot{x}_e + J\dot{q}\|^2 + \lambda\|\dot{q}\|^2\} \quad (2.45)$$

where  $\lambda$  is damped factor. The solution of inverse kinematic equation (2.43) with optimal function (2.45) given

$$\dot{q} = J^T(JJ^T + \lambda^2 I + \alpha^2 \hat{u}_m \hat{u}_m^T)^{-1} \dot{x}_e \quad (2.46)$$

In this case,  $J^\#(q) = J^T(JJ^T + \lambda^2 I + \alpha^2 \hat{u}_m \hat{u}_m^T)^{-1}$ .

Procedure: Solving inverse kinematic

**Step 1** Finding SVD<sup>1</sup> of the Jacobian matrix  $J$

$$J = UDV^T$$

where  $U \in \mathbb{R}^{m \times n}$  and  $V \in \mathbb{R}^{n \times n}$  are orthogonal matrices.  $D \in \mathbb{R}^{m \times n}$  is a matrix with all non-diagonal entries equal to zero and with the diagonal entries  $D_{i,j} = \sigma_i$  with  $\sigma_1 \geq \sigma_2 \geq \dots \geq \sigma_m \geq 0$

**Step 2** Choose weight factors  $\lambda_{max}$ ,  $\alpha$  and  $\epsilon$

**Step 3**  $\hat{u}_m$  is column  $m$ -th of matrix  $U$

**Step 4** Calculate damped factor

$$\lambda = \begin{cases} \left[1 - \left(\frac{\sigma_m}{\epsilon}\right)^2\right] \lambda_{max} & \text{if } \sigma_m < \epsilon \\ \lambda_{max} & \text{if } \sigma_m \geq \epsilon \end{cases}$$

**Step 5** The discrete form of equations (2.46)

$$\Delta q = J^T(JJ^T + \lambda^2 I + \alpha^2 \hat{u}_m \hat{u}_m^T)^{-1} \Delta x_e$$

Figure 2.12 shows the result when one leg in singular posture with  $rank(J) = 4$ , after 60-th iteration  $e \approx 3.6 \times 10^{-10}$ , robot can move to desired position.

---

<sup>1</sup> Singular Value Decomposition

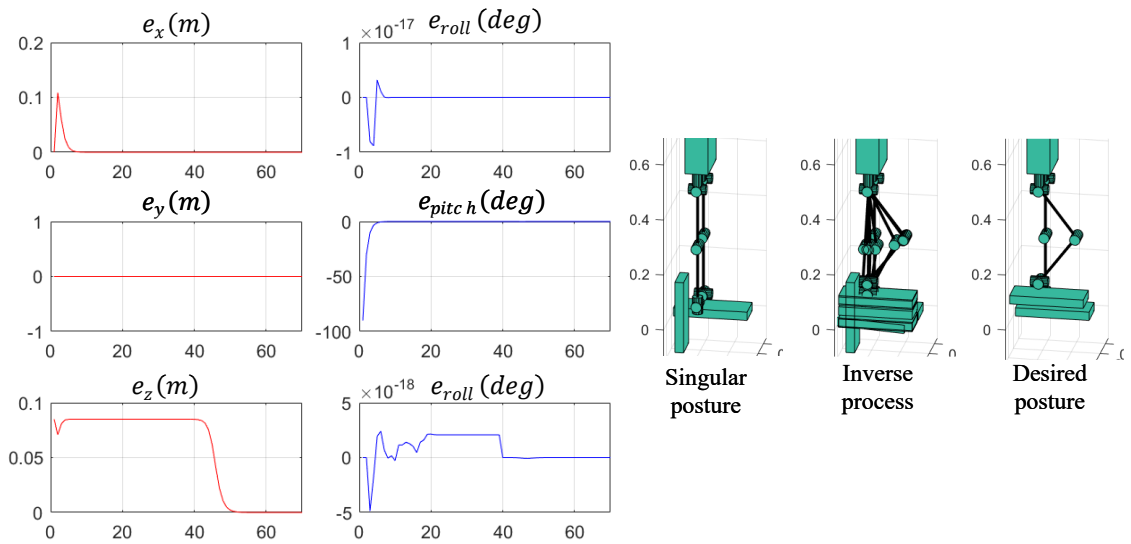


**Figure 2.12** Inverse kinematic of a singular posture.

## CHAPTER 3: CONTROL OF WALKING GAIT

The human gait consists of a repeatable cycle which is described by two phases: a double support phase (DSP) and a single-support phase (SSP). The cycle starts the foot becomes the rearmost foot leaves the ground and becomes the front foot again. During the double-support phase, both feet are in contact with the ground. During the single support phase, while one foot is stationary on the ground, the other foot swings from the rear to the front.

In this section, we implement our method to design CoM and ankles trajectories adapt with human walking gait

### 3.1 CoM trajectory

Let us recall the method biped walking pattern generation by using preview control of ZMP was proposed by S. Kajita [27]. We define a new variable  $u_x$  as the time derivative of the horizontal acceleration of CoM.

$$\frac{d}{dt} \ddot{x} = u_x \quad (3.1)$$

By using this input, we can rewrite the ZMP (in  $x$  direction) equation (2.30) into the following state space representation

$$\begin{aligned} \frac{d}{dt} \begin{bmatrix} x \\ \dot{x} \\ \ddot{x} \end{bmatrix} &= \begin{bmatrix} 0 & 1 & 0 \\ 0 & 0 & 1 \\ 0 & 0 & 0 \end{bmatrix} \begin{bmatrix} x \\ \dot{x} \\ \ddot{x} \end{bmatrix} + \begin{bmatrix} 0 \\ 0 \\ 1 \end{bmatrix} u_x \\ p_x(k) &= [1 \ 0 \ -z_c/g] \begin{bmatrix} x \\ \dot{x} \\ \ddot{x} \end{bmatrix} \end{aligned} \quad (3.2)$$

From equation (3.4), we can construct a walking pattern generator as a ZMP tracking control system given by Figure 3.1.

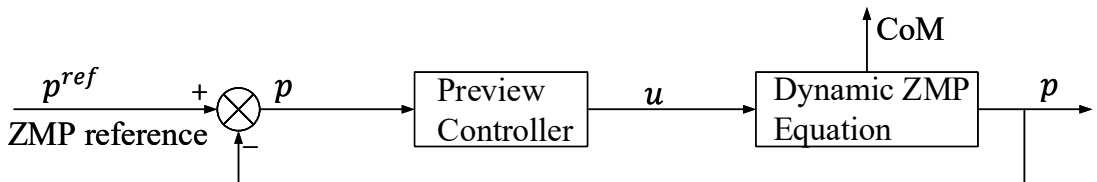


**Figure 3.1** Pattern generation as ZMP tracking control

Discretization equation (3.2) of system with sampling time  $\Delta t$  as

$$\begin{aligned} x(k+1) &= Ax(k) + Bu(k) \\ p(k) &= Cx(k) \end{aligned} \quad (3.3)$$

Where:

$$\begin{aligned} x(k) &= [x(k\Delta t) \ \dot{x}(k\Delta t) \ \ddot{x}(k\Delta t)]^T \\ u(k) &= u_x(k\Delta t) \\ p(k) &= p_x(k\Delta t) \\ A &= \begin{bmatrix} 1 & \Delta t & \Delta t^2/2 \\ 0 & 1 & \Delta t \\ 0 & 0 & 1 \end{bmatrix} \\ B &= [\Delta t^3/6 \ \Delta t^2/2 \ \Delta t]^T \\ C &= [1 \ 0 \ -z_c/g] \end{aligned}$$

With the given reference of ZMP in x direction  $p_x^{ref}(k)$ , the performance index for optimal preview servo controller

$$J = \sum_{i=k}^{\infty} \{Q_e e(i)^2 + \Delta t^T(i) Q_x \Delta x(i) + R \Delta u^2(i)\} \quad (3.4)$$

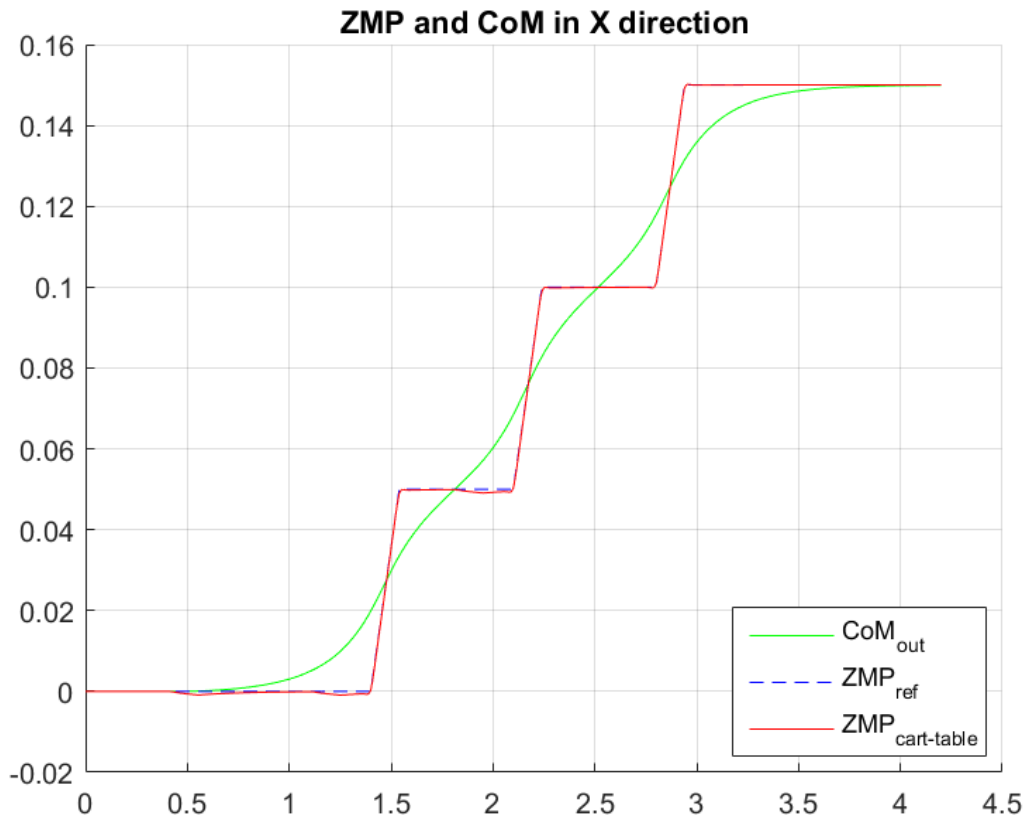
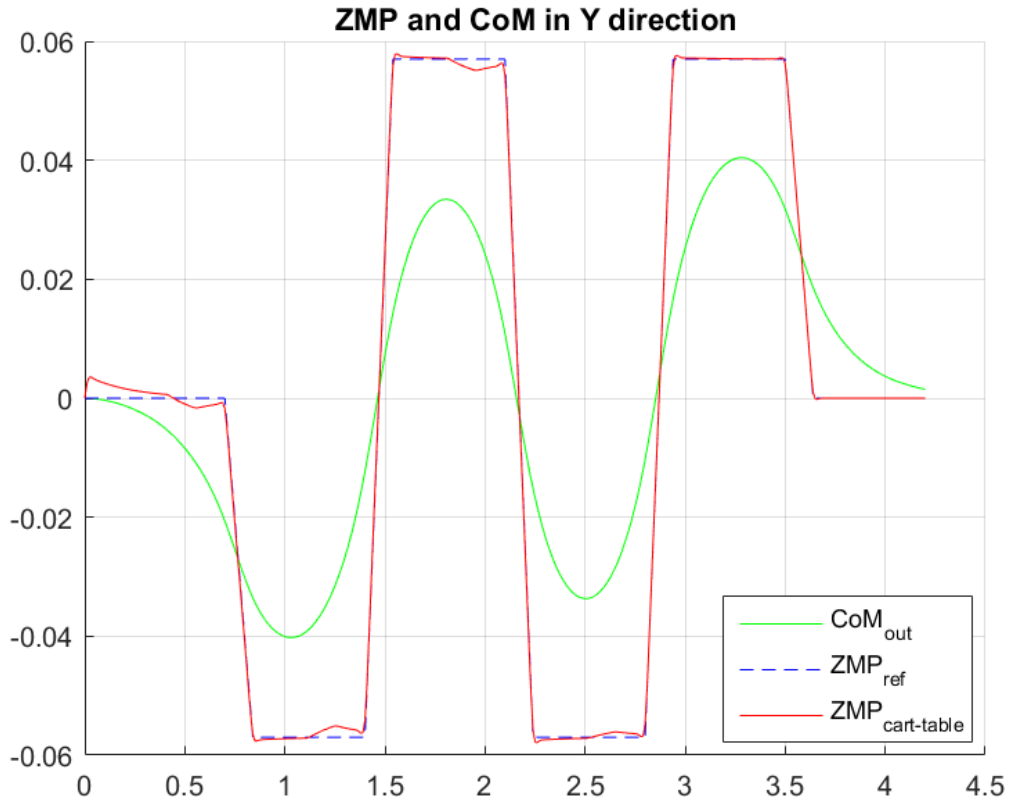
where  $e(i) = p_x(i) - p_x^{ref}(i)$  is servo error,  $Q_e, R > 0$  and  $Q_x$  is a  $3 \times 3$  symmetric non-negative definite matrix.  $\Delta x(k) = x(k) - x(k-1)$  is the incremental state vector and  $\Delta u(k) = u(k) - u(k-1)$  is the incremental input.

When the ZMP reference can be previewed for  $N_L$  step future at every sampling time, the optimal controller is given by

$$u(k) = -G_i \sum_{i=0}^k e(k) - G_x x(k) - \sum_{j=1}^{N_L} G_p(j) p_x^{ref}(k+j) \quad (3.5)$$

where  $G_i$ ,  $G_x$  and  $G_p(j)$  are the gains calculated from the weights  $Q_e, Q_x, R$  and the system parameter.

Figure 3.4 shows CoM trajectory was calculated by preview control with  $\Delta t = 10ms$ ,  $N_L = 10$ .

**Figure 3.2** ZMP reference and CoM trajectory on *x* direction**Figure 3.3** ZMP reference and CoM trajectory on *y* direction

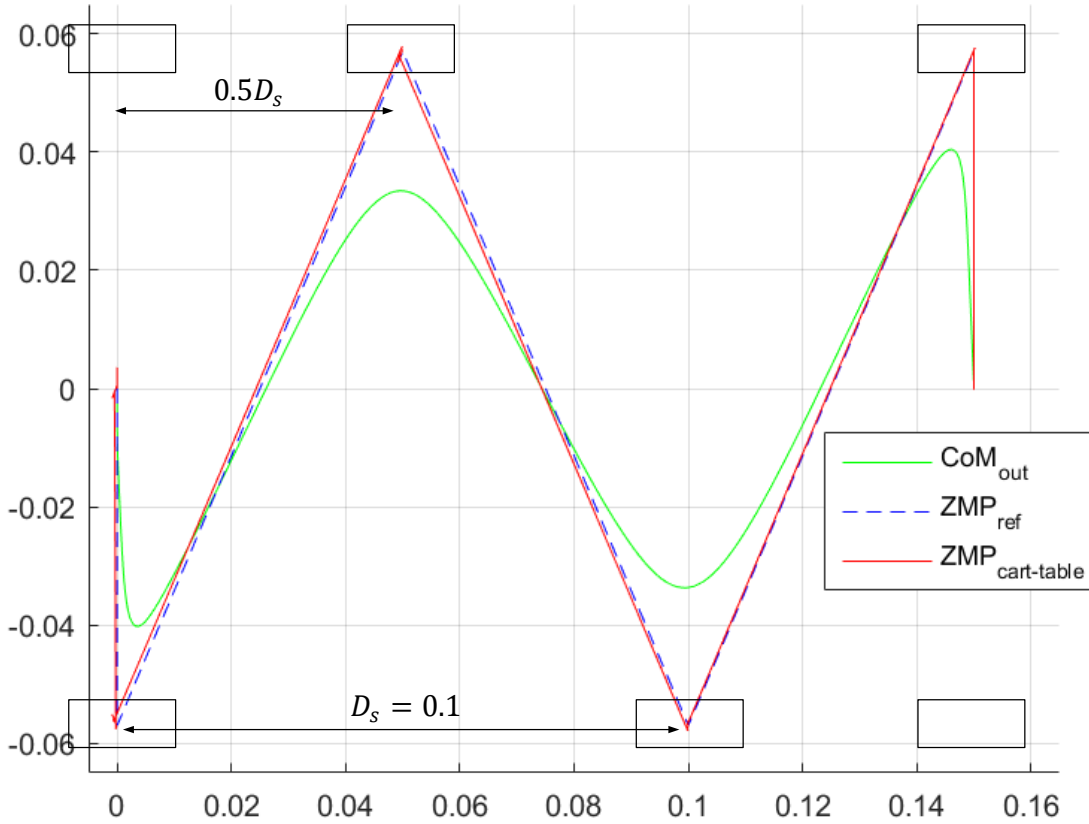


**Figure 3.4** Footstep planning, ZMP reference and CoM trajectory in  $xy$  plan

### 3.1 Ankle trajectory

While robot is walking, we assume that foot not rotate. From foot step planning at Figure 3.4, we created ankles trajectory by interpolation-based method.

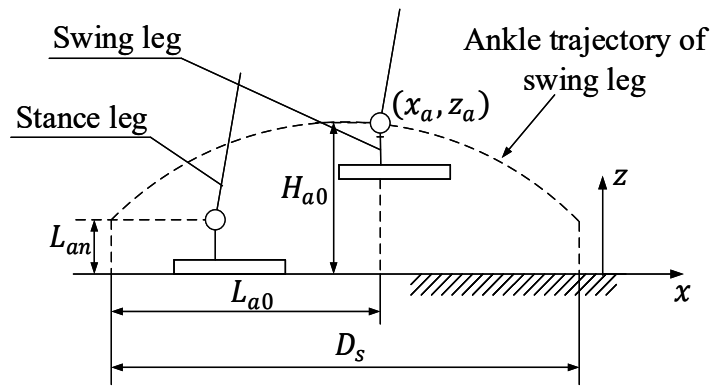


**Figure 3.5** Ankle trajectories design with  $L_{a0} = D_s/2$ ,  $H_{a0} = 0.03 \text{ m}$ ,  $L_{an} = l_5$ .

## CONTROL OF WALKING GAIT

In swing phase, ankle position in  $z$  ( $z_a$ ) and  $x$  ( $x_a$ ) direction are described by forth order polynomials  $f(t) = a_1t^4 + a_2t^3 + a_3t^2 + a_4t + a_5$  with the boundary conditions as

$$\begin{cases} x_a(t_0) = x_n \\ x_a(t_0 + T_{sw}/2) = x_n + L_{a0} \\ x_a(t_0 + T_{sw}) = x_n + D_s \\ \dot{x}_a(t_0) = 0 \\ \dot{x}_a(t_0 + T_{sw}) = 0 \end{cases} \quad (3.6)$$

$$\begin{cases} z_a(t_0) = L_{an} \\ z_a(t_0 + T_{sw}/2) = H_{a0} \\ z_a(t_0 + T_{sw}) = L_{an} \\ \dot{z}_a(t_0) = 0 \\ \dot{z}_a(t_0 + T_{sw}) = 0 \end{cases} \quad (3.7)$$

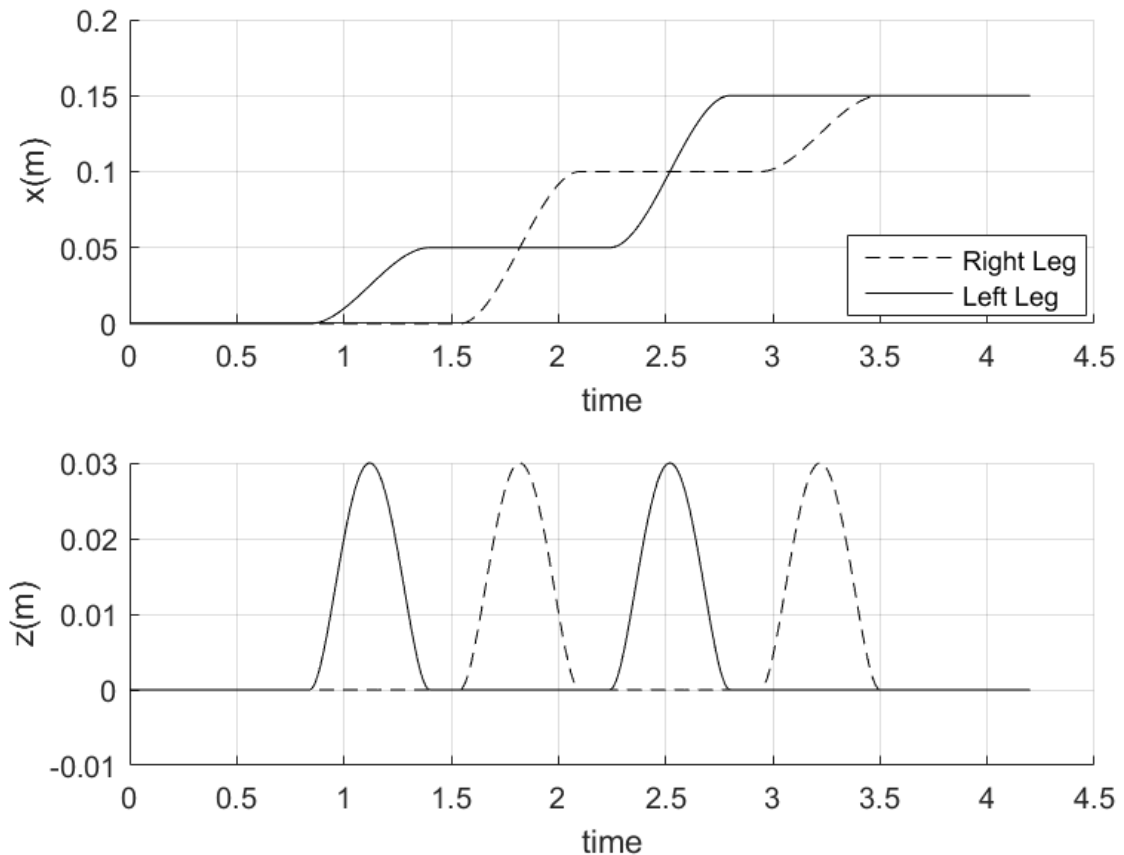


**Figure 3.6** Walking gait of 4 steps with single support, double support, swing, stance phase time are:  $T_{ss} = 0.56\text{ s}$ ,  $T_{ds} = 0.14\text{ s}$ ,  $T_{sw} = 0.56\text{ s}$ ,  $T_{st} = 0.84\text{ s}$

## CHAPTER 4: SIMULATION AND EXPERIMENT

In this chapter, by using the trajectories was generated, the simulation model will performance a straight walking then these trajectories are applied to real model UXA-90 robot. The results show difference of simple, multibody model and real robot.

### 4.1 Simulation

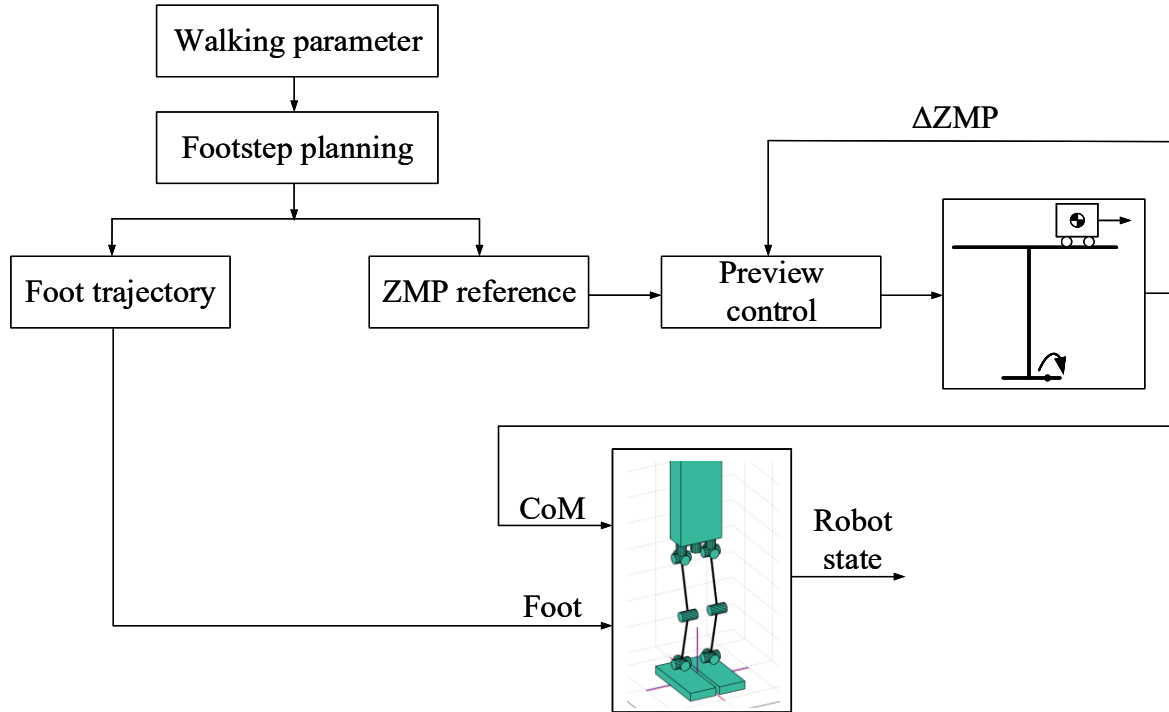


**Figure 4.1** The block diagram of biped robot walking simulation

Figure 4.1 shows the biped walking simulation process, the inputs of simulation are: CoM and Foot trajectories were designed in Chapter 3. This tool is written on MATLAB, it evaluates the robot state before we apply to real model. During robot walking, joint trajectories of biped legs are given in Figure 4.2.

## SIMULATION AND EXPERIMENT

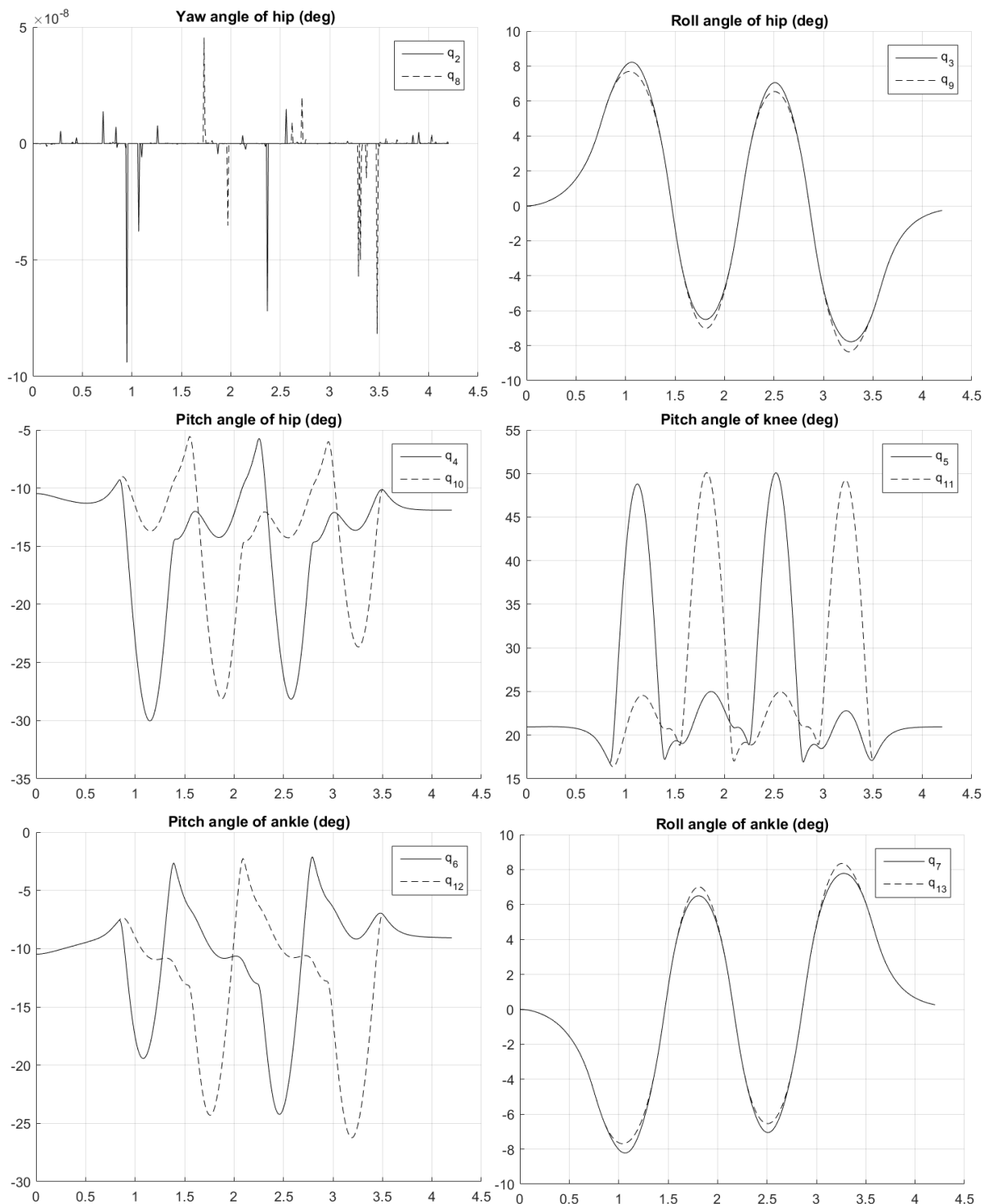


**Figure 4.2** Joints position during walk

## 4.2 Experiment on UXA-90 robot

### 4.2.1 ZMP module

In order to review the stable of walking gait, we design a simple ZMP module using force sensor on each foot. The design showed in Figure 4.3 and Figure 4.4.

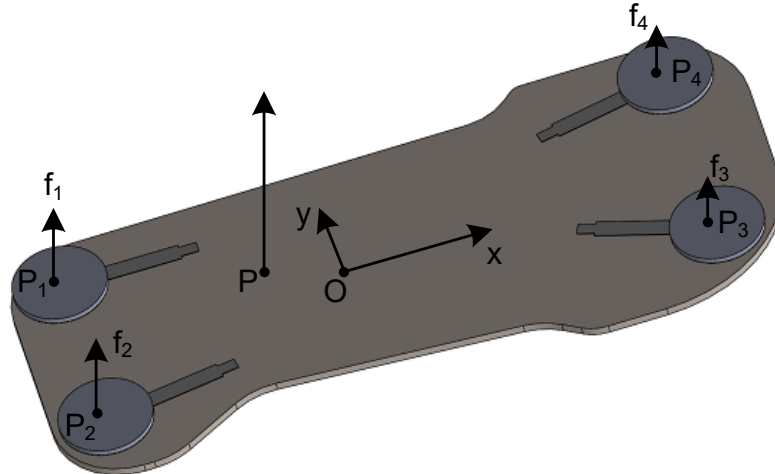


**Figure 4.3** Configuration of 4 sensors on each foot

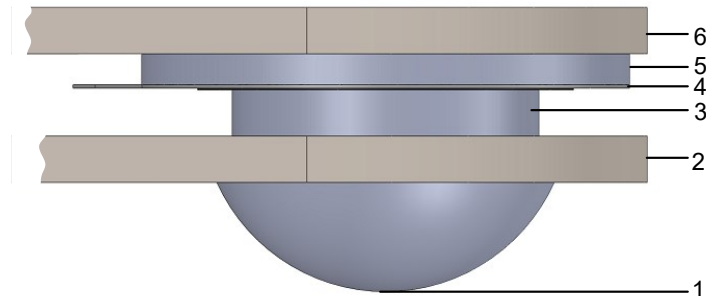


**Figure 4.4** Attachment of each sensor include: (1) Contact point; (2) Foot plate 1; (3) Rigid plate 1; (4) Rigid plate 2; (5) Flexi Force A401 sensor; (6) Foot plate 2

In this design, using data from sensors, ZMP on each leg is calculated

$$P_x = \frac{\sum_{i=1}^4 (P_{ix} \cdot f_i)}{\sum_{i=1}^4 f_i}$$

$$P_y = \frac{\sum_{i=1}^4 (P_{iy} \cdot f_i)}{\sum_{i=1}^4 f_i} \quad (4.1)$$

During walking, magnitude of pressure on each foot show in Figure 4.5

## SIMULATION AND EXPERIMENT

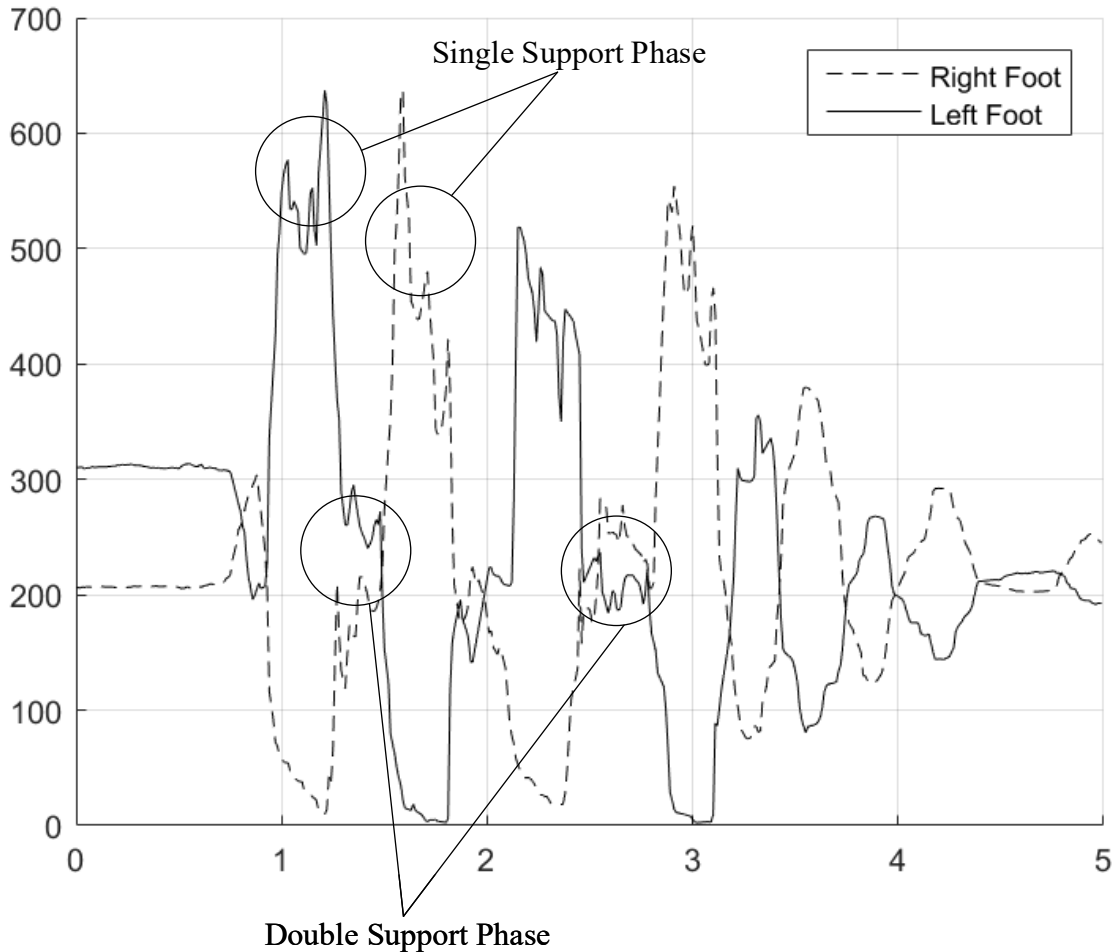


**Figure 4.5** Magnitude of pressure

### 4.2.2 Experiment results and discussion

To get a successful walking gait on UXA-90 robot, we have to redesign walking gait when robot falling down. Figure 4.6 and Figure 4.7 show the result of a successful walking gait on robot UXA-90. By using ZMP module, we can analysis the stability of robot during walk.

The ZMP of real model is different with simulation model, this result showed that simulation model should be modified accurately and ZMP sensor have to be calibrated. In the future, a dynamic model of biped robot should be developed with accurate dynamic parameter of UXA-90 robot.

## SIMULATION AND EXPERIMENT

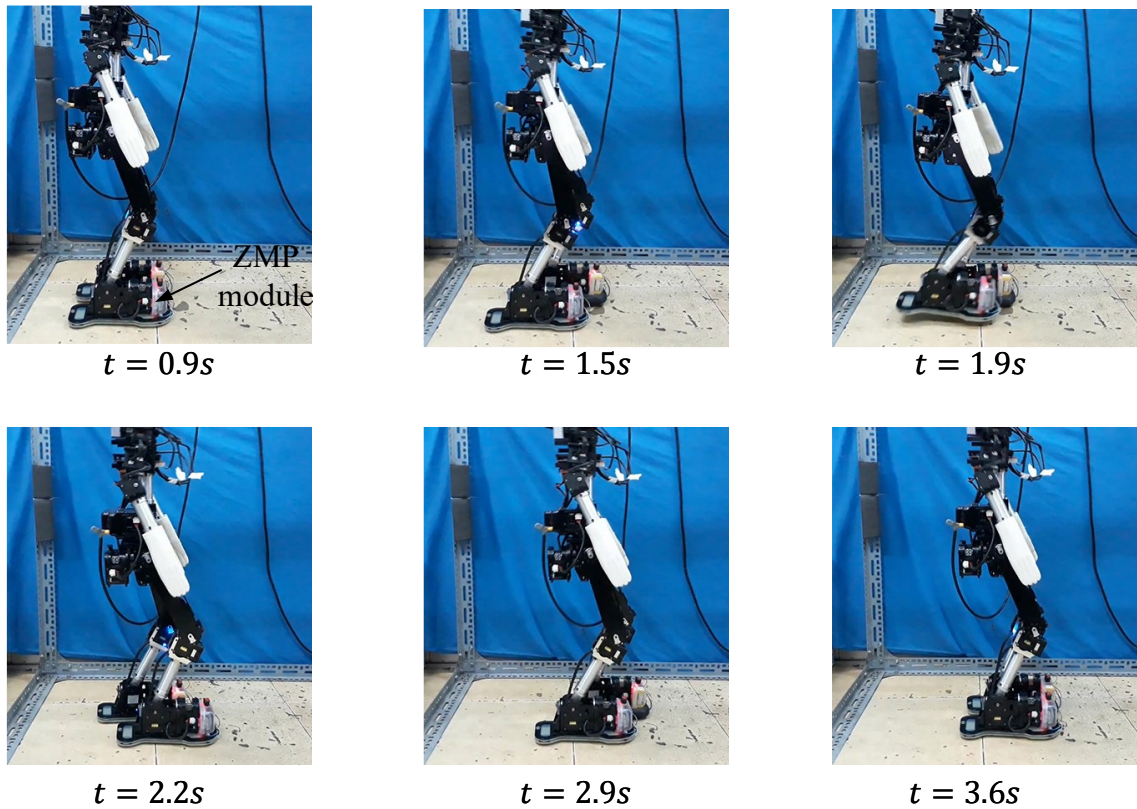


**Figure 4.6** Implement walking gait on real robot

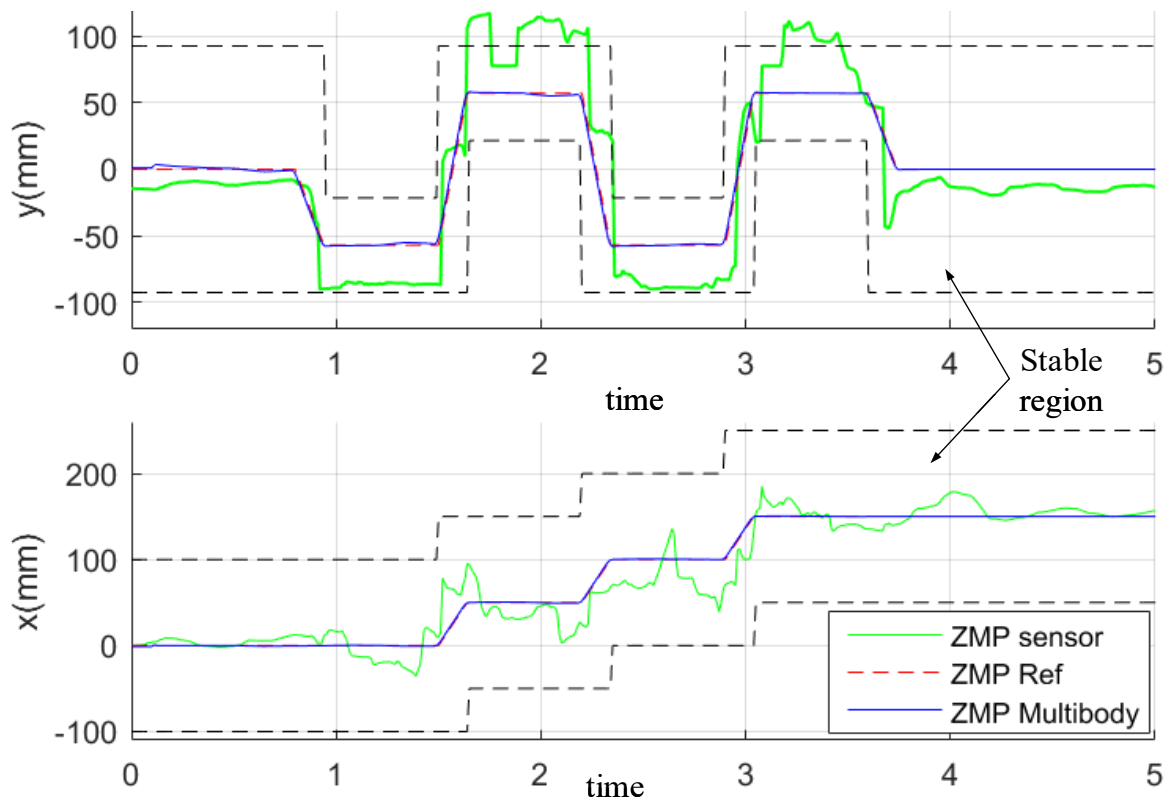


**Figure 4.7** Simulation and experiment result of ZMP

## SIMULATION AND EXPERIMENT

The real ZMP does not tracking well to the desired trajectory. The controller of UXA-90 robot is open-loop, ZMP module uses to review the stable of walking gait was designed. A tracking controller should be applied to make robot walking more stable, it makes ZMP tracks following the reference trajectory accurately.

## CHAPTER 5: CONCLUSION

This thesis is a part of project: Study on design and manufacturing Humanoid robot for promotion service, which funded by Ho Chi Minh city DOST. At the first step, the purposes of project are understanding structure and controller system of humanoid robot based on robot UXA-90. Next step, project will release a humanoid robot platform and it is used for promotion service. These conclusions are evaluating study on robot UXA-90 and recommendation for future research.

### 5.1 Remark of UXA-90

UXA-90 is a multipurpose humanoid robot platform for Research/Education/Exhibition/Performance, however it is being developed. UXA-90 doesn't have any ZMP module on foot, IMU sensor is not connected to sub controller. By default, it contains some motions stored in sub-controller's memory, these motions are encrypted and can't modify.

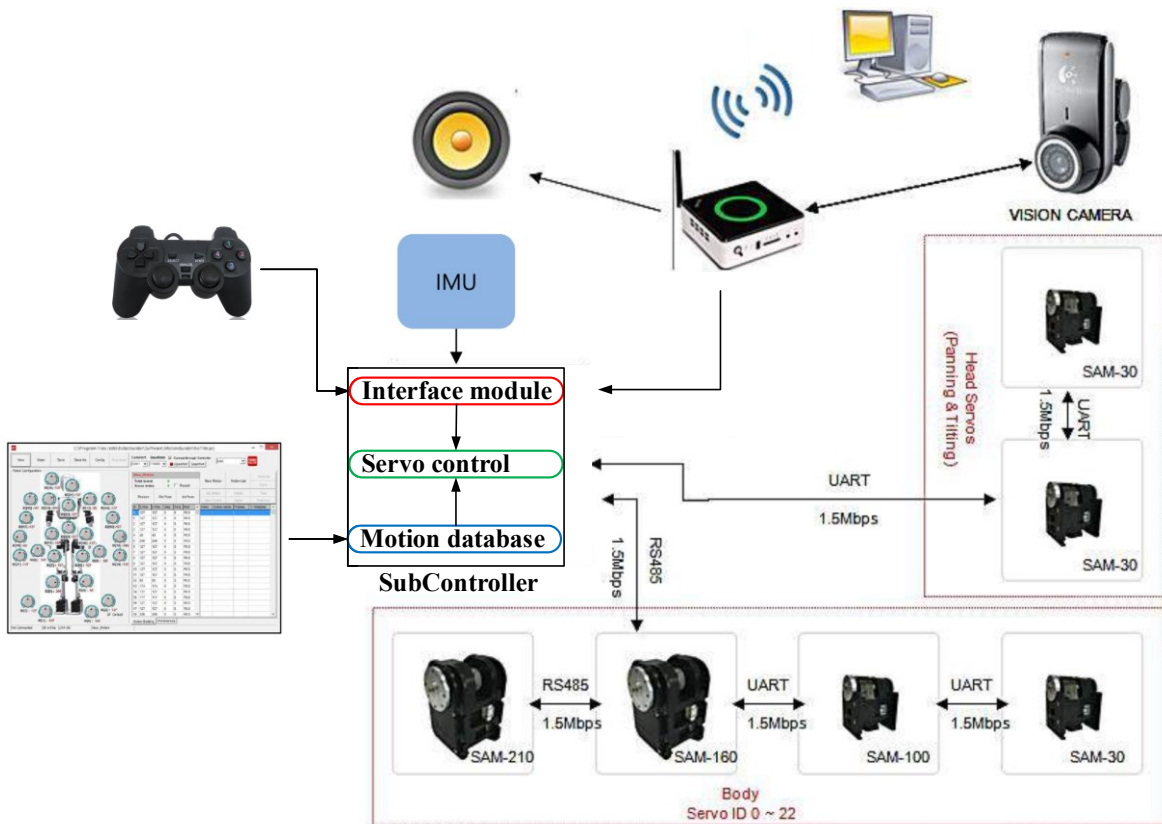


Figure 5.1 System schematic of robot UXA-90

To control UXA-90 humanoid robot we have two methods

- Using Robobuilder software to create motion then store in motion database
- Using interface module to control all joints of robot

### 5.2 Contributions of thesis

Through this research, the following technical objectives were achieved:

- The forward and inverse kinematic of 12 DoF biped robot were solved.
- A simulation model was built to evaluate biped walking performance.
- A stable walking gait was designed and experment.

### 5.3 Recommendations for future research

From the experience gained during this thesis, several suggestions for future research on biped walking robots can be made

#### Trajectory generation

This thesis only generates trajectory for straight walk. Future research should performances circle walk, generate trajectory for upper body (hands, head), create some basic motions: sit down, stand up, shake hands.

#### Stabilizing control

Because UXA-90 robot is being developed, all the motion controllers are open-loop. Future research should integrate IMU sensor for balancing and ZMP module for dynamic stable walking.

#### ROS framework

ROS<sup>1</sup> is a collection of software frameworks for robot software development, providing operating system-like functionality on a heterogeneous computer cluster. ROS provides standard operating system services such as hardware abstraction, low-level device control, implementation of commonly used functionality, message-passing between processes, and package management.

---

<sup>1</sup> Robot Operating System

## CHAPTER 5: CONCLUSION

Many humanoid projects develop robot software based on ROS frameworks: HRP, Hubo, Atlas..., future research should integrate ROS for software system of robot UXA-90.

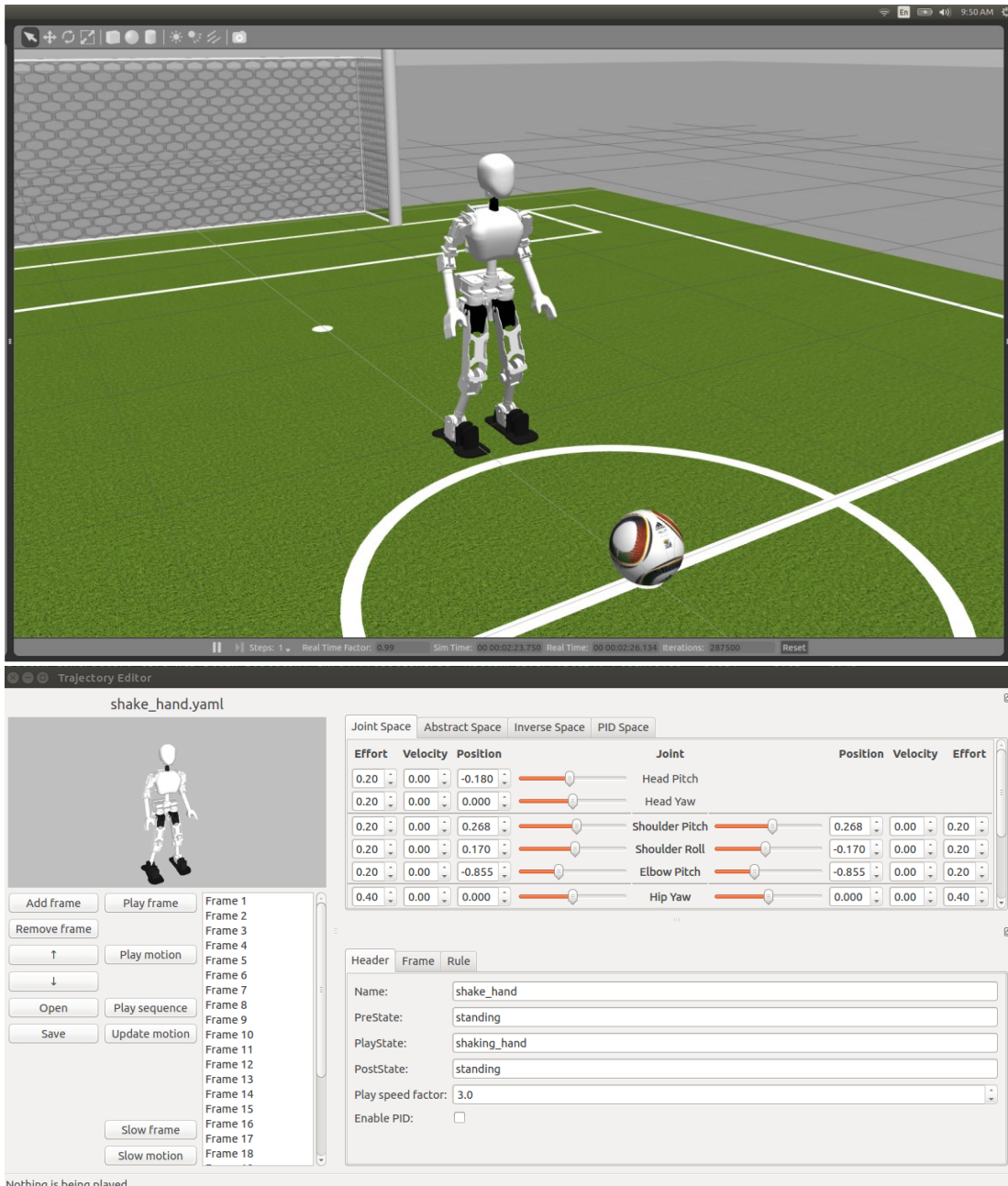


**Figure 5.2** ROS software is being developed by author

## References

- [1] I. Kato and H. Tsuiki, “The hydraulically powered biped walking machine with a high carrying capacity,” in *Proc. of the 4th International Symposium on External Control of Human Extremities*, 1972, pp. 410–421.
- [2] K. Kaneko *et al.*, “Design of prototype humanoid robotics platform for HRP,” in *IEEE/RSJ International Conference on Intelligent Robots and Systems, 2002*, 2002, vol. 3, pp. 2431–2436 vol.3.
- [3] Y. Ogura, H. Aikawa, K. Shimomura, A. Morishima, H. Lim, and A. Takanishi, “Development of a new humanoid robot WABIAN-2,” in *Robotics and Automation, 2006. ICRA 2006. Proceedings 2006 IEEE International Conference on*, 2006, pp. 76–81.
- [4] K. Hirai, M. Hirose, Y. Haikawa, and T. Takenaka, “The development of Honda humanoid robot,” in *Robotics and Automation, 1998. Proceedings. 1998 IEEE International Conference on*, 1998, vol. 2, pp. 1321–1326.
- [5] M. Hirose and K. Ogawa, “Honda humanoid robots development,” *Philos. Trans. R. Soc. Math. Phys. Eng. Sci.*, vol. 365, no. 1850, pp. 11–19, Jan. 2007.
- [6] H. Hirukawa *et al.*, “Humanoid robotics platforms developed in HRP,” *Robot. Auton. Syst.*, vol. 48, no. 4, pp. 165–175, Oct. 2004.
- [7] K. Yokoi, F. Kanehiro, K. Kaneko, K. Fujiwara, S. Kajita, and H. Hirukawa, “A honda humanoid robot controlled by aist software,” in *Proc. of the IEEE-RAS International Conference on Humanoid Robots*, 2001, pp. 259–264.
- [8] K. Kaneko, K. Harada, F. Kanehiro, G. Miyamori, and K. Akachi, “Humanoid robot HRP-3,” in *Intelligent Robots and Systems, 2008. IROS 2008. IEEE/RSJ International Conference on*, 2008, pp. 2471–2478.
- [9] K. Kaneko *et al.*, “Humanoid robot hrp-4-humanoid robotics platform with lightweight and slim body,” in *Intelligent Robots and Systems (IROS), 2011 IEEE/RSJ International Conference on*, 2011, pp. 4400–4407.
- [10] J. Kim, S. Park, I. Park, and J. Oh, “Development of a humanoid biped walking robot platform khr-1-initial design and its performance evaluation,” *feedback*, vol. 1, pp. 1–12, 2002.
- [11] J.-Y. Kim, I.-W. Park, J. Lee, M.-S. Kim, B.-K. Cho, and J.-H. Oh, “System design and dynamic walking of humanoid robot KHR-2,” in *Robotics and Automation, 2005. ICRA 2005. Proceedings of the 2005 IEEE International Conference on*, 2005, pp. 1431–1436.
- [12] I.-W. Park, J.-Y. Kim, J. Lee, and J.-H. Oh, “Online free walking trajectory generation for biped humanoid robot KHR-3 (HUBO),” in *Robotics and Automation, 2006. ICRA 2006. Proceedings 2006 IEEE International Conference on*, 2006, pp. 1231–1236.

## References

- [13] G. Nelson *et al.*, “Petman: A humanoid robot for testing chemical protective clothing,” *日本ロボット学会誌*, vol. 30, no. 4, pp. 372–377, 2012.
- [14] G. M. Atmeh, I. Ranatunga, D. O. Popa, K. Subbarao, F. Lewis, and P. Rowe, “Implementation of an adaptive, model free, learning controller on the Atlas robot,” in *American Control Conference (ACC), 2014*, 2014, pp. 2887–2892.
- [15] N. A. Radford *et al.*, “Valkyrie: NASA’s First Bipedal Humanoid Robot,” *J. Field Robot.*, vol. 32, no. 3, pp. 397–419, 2015.
- [16] “Gait in prosthetic rehabilitation - Physiopedia, universal access to physiotherapy knowledge.” [Online]. Available: [http://www.physio-pedia.com/Gait\\_in\\_prosthetic\\_rehabilitation](http://www.physio-pedia.com/Gait_in_prosthetic_rehabilitation). [Accessed: 09-May-2016].
- [17] M. Vukobratović and B. Borovac, “Zero-moment point — thirty five years of its life,” *Int. J. Humanoid Robot.*, vol. 01, no. 01, pp. 157–173, Mar. 2004.
- [18] S. Kajita, H. Hirukawa, K. Harada, and K. Yokoi, *Introduction to Humanoid Robotics*, vol. 101. Berlin, Heidelberg: Springer Berlin Heidelberg, 2014.
- [19] H. F. N. Al-Shuka, F. Allmendinger, B. Corves, and W.-H. Zhu, “Modeling, stability and walking pattern generators of biped robots: a review,” *Robotica*, vol. 32, no. 06, pp. 907–934, Sep. 2014.
- [20] W. Yang, N. Young, and B.-J. You, *Biologically Inspired Robotic Systems Control: Multi-DOF Robotic Arm Control*. Saarbrücken: VDM Verlag Dr. Müller, 2010.
- [21] P. van Zutven, D. Kostić, and H. Nijmeijer, “On the stability of bipedal walking,” in *Simulation, modeling, and programming for autonomous robots*, Springer, 2010, pp. 521–532.
- [22] M. Hackel, *Humanoid robots: human-like machines*. Vienna: Advanced Robotic Systems International : I-Tech, 2007.
- [23] M. Vukobratović and J. Stepanenko, “On the stability of anthropomorphic systems,” *Math. Biosci.*, vol. 15, no. 1, pp. 1–37, Oct. 1972.
- [24] S. Kajita, F. Kanehiro, K. Kaneko, K. Yokoi, and H. Hirukawa, “The 3D linear inverted pendulum mode: a simple modeling for a biped walking pattern generation,” in *2001 IEEE/RSJ International Conference on Intelligent Robots and Systems, 2001. Proceedings*, 2001, vol. 1, pp. 239–246 vol.1.
- [25] B. Siciliano, L. Sciavicco, and G. Oriolo, *Robotics: Modelling, Planning and Control*, 1st ed. 2009 edition. London: Springer, 2011.
- [26] A. A. Maciejewski and C. A. Klein, “Numerical filtering for the operation of robotic manipulators through kinematically singular configurations,” *J. Field Robot.*, vol. 5, no. 6, pp. 527–552, 1988.
- [27] S. Kajita *et al.*, “Biped walking pattern generation by using preview control of zero-moment point,” in *Robotics and Automation, 2003. Proceedings. ICRA ’03. IEEE International Conference on*, 2003, vol. 2, pp. 1620–1626.

## Appendix A: MATLAB code

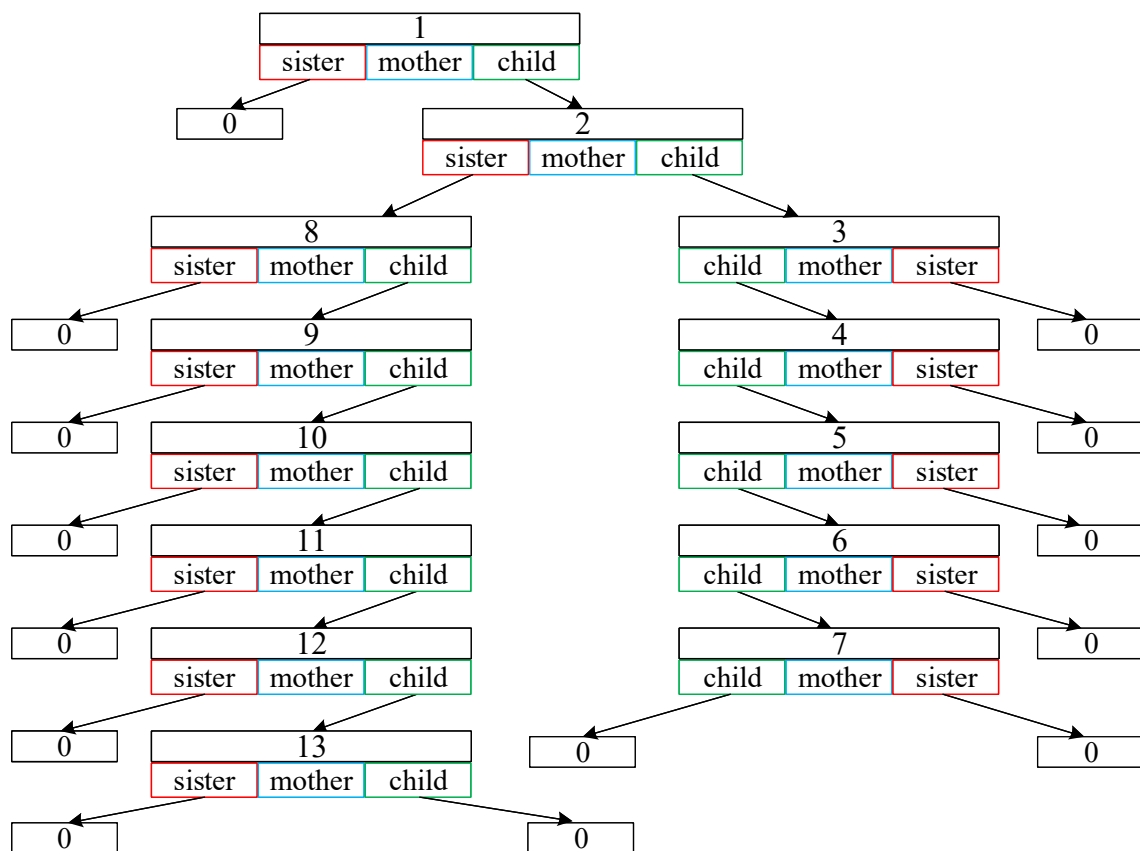


**Figure A.1** The binary tree of robot link

The list of MATLAB simulation function and script\*

<https://github.com/nvtienanh/masterthesis>

<b>function</b>	<i>setup_system_path.m</i>
Adding all sub folder to MATLAB workspace	
<b>script</b>	<i>SetupBipedRobot.m</i>
Construction robot model	
<b>function</b>	<i>FindMother.m</i>

\* Some functions are inherited from textbook [18]

## Appendix A

Finding the kinematic chain	
<b>function</b>	<i>SetupRigidBody.m</i>
Setting 3D model of robot link	
<b>function</b>	<i>ForwardKinematics.m</i>
Calculating forward kinematic of robot	
<b>function</b>	<i>TotalMass.m</i>
Calculating the total of mass	
<b>function</b>	<i>FindRoute.m</i>
List all link in a kinematic chain	
<b>function</b>	<i>CalcJacobian.m</i>
Calculating the Jacobian matrix of kinematic chain	
<b>function</b>	<i>MoveJoints.m</i>
Move a joint to new position	
<b>function</b>	<i>CalcVWerr.m</i>
Calculating the posture error	
<b>function</b>	<i>ikine_sdls.m</i>
Calculating the inverse kinematic	
<b>function</b>	<i>PatternGenerator.m</i>
Designing walking gait	
<b>function</b>	<i>CalStanceFootPlace.m</i>
Calculating footstep placement	
<b>function</b>	<i>UXA_Ankle_X.m</i>
Interpolating the ankle position in x direction	
<b>function</b>	<i>UXA_Ankle_Z.m</i>
Interpolating the ankle position in z direction	
<b>function</b>	<i>calc_preview_controller.m</i>
Calculating preview controller	
<b>function</b>	<i>ForwardVelocity.m</i>
Calculating the velocities of robot link	

## Appendix A

<b>function</b>	<i>calcCoM.m</i>
Calculating Center of Mass	
<b>function</b>	<i>calcP.m</i>
Calculating the linear momentum	
<b>function</b>	<i>calcL.m</i>
Calculating the angular momentum	
<b>function</b>	<i>calcZMP.m</i>
Calculating the ZMP or robot	
<b>function</b>	<i>DrawAllJoints.m</i>
Drawing robot model	
<b>script</b>	<i>UXA_IK_demo.m</i>
Inverse kinematic demo	
<b>script</b>	<i>UXA_IK_demo_2.m</i>
Inverse kinematic demo (using function ikne_sdls)	
<b>script</b>	<i>UXA_FK_demo.m</i>
Forward kinematic demo	
<b>function</b>	<i>Dhmod.m</i>
Calculating the Modified DH of robot link	
<b>script</b>	<i>UXA_PreviewControl.m</i>
Robot simulation file	
<b>script</b>	<i>UXA_PatternGenerator_demo.m</i>

## Appendix B

### Appendix B: UXA-90 datasheet

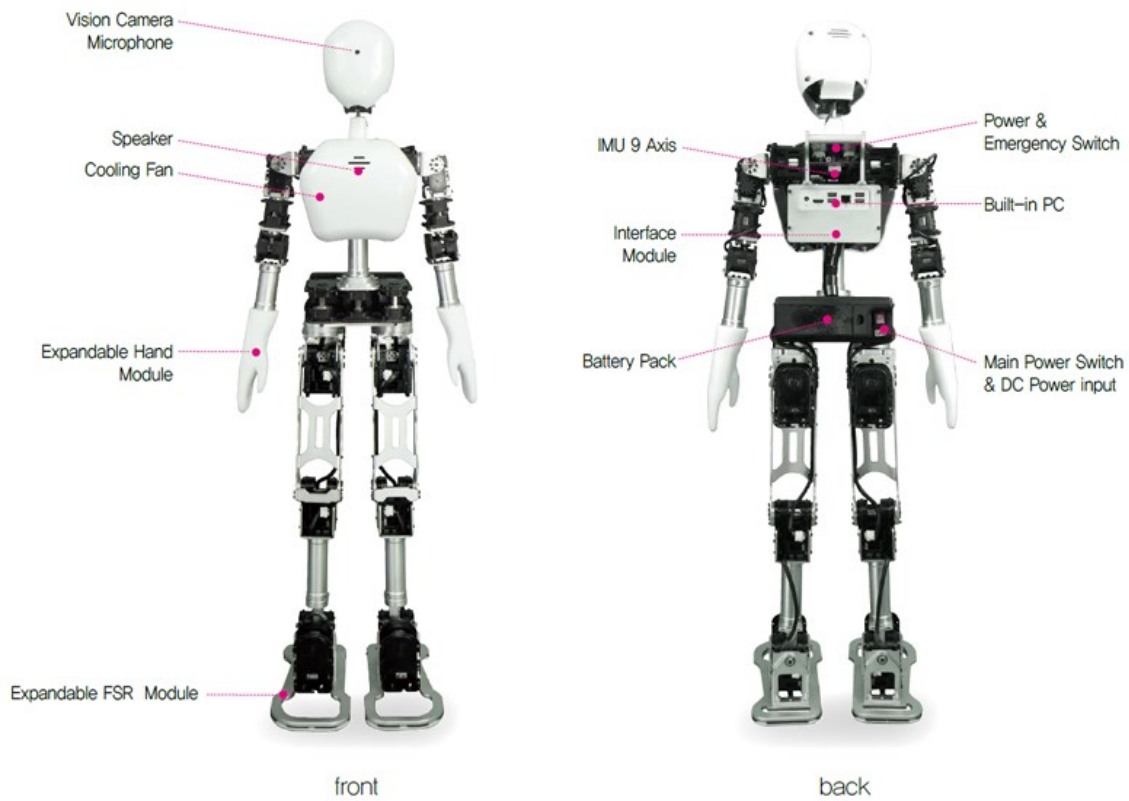


**Figure A.2** UXA-90 specifications

#### Robot UXA-90 specifications

Weight	9.5 kg
Height	1 m
Width	0.35 m
DOF	23 DOF in total: 12 DOF for legs 8 DOF arms 1 DOF for waist 2 DOF for head
Sensor	IMU 2G 9Axis, $\pm 180^\circ\text{C}$ (Roll/Yaw), $\pm 90^\circ\text{C}$ (Pitch)
Wireless	802.11 b/g/n
External interface	USB2.0 x 2 , Ethernet 10/100/1000 Base T USB3.0 x 2, HDMI x 1

## Appendix B

Speaker	1 ea.
Microphone	1 ea.
Vision Camera	Logitech C905 / HD 1600x1200 pixel
Battery	Lithium Polymer 18.5V, 2250mA
OS	Window7 Linux Ubuntu 14.04



Model	SAM-30
Max Torque(kgf.Cm)	28 at 19V/2A
Max speed(rpm)	90
Gear material	Metal
Resoulution(degree)	1.08° (Quick mode) 0.083° (Standard mode)
Network Interface	UART Serial (Multi drop TTL full duplex)
Operation voltage(V)	14~24
Position sensor	POT(340°)

Model	SAM-100P
Max Torque(kgf.Cm)	100 at 24V/5A
Max speed(rpm)	65
Gear material	Metal
Resoulution(degree)	1.08° (Quick mode) 0.083° (Standard mode)
Network Interface	RS-485 Half duplex / UART Serial (Multi drop TTL full duplex)
Operation voltage(V)	14~24
Position sensor	Optical Enc(358°) + POT(340°)

**Figure A.3** SAM-30 and SAM-100P specifications



Model	SAM-160P
Max Torque(kgf.Cm)	160 at 24V/5A
Max speed(rpm)	40
Gear material	Metal
Resoulution(degree)	1.08° (Quick mode) 0.083° (Standard mode)
Network Interface	RS-485 Half duplex / UART Serial (Multi drop TTL full duplex)
Operation voltage(V)	14~24
Position sensor	Optical Enc(358°) + POT(340°)

Model	SAM-210P
Max Torque(kgf.Cm)	210 at 24V/5A
Max speed(rpm)	30
Gear material	Metal
Resoulution(degree)	1.08° (Quick mode) 0.083° (Standard mode)
Network Interface	RS-485 Half duplex / UART Serial (Multi drop TTL full duplex)
Operation voltage(V)	14~24
Position sensor	Optical Enc(358°) + POT(340°)

**Figure A.4** SAM-160P and SAM-210P specifications

**Publications**